# A deterministic, age-stratified, extended SEIRD model for investigating the effect of non-pharmaceutical interventions on SARS-CoV-2 spread in Belgium.

Tijs W. Alleman[1,*], Jenna Vergeynst[1,2], Elena Torfs[1], Daniel Illana[1], Ingmar Nopens[1], and Jan Baetens[2]

[1]*BIOMATH, Department of Data Analysis and Mathematical Modelling, Ghent University, Coupure links 653, 9000 Gent, Belgium*
[2]*KERMIT, Department of Data Analysis and Mathematical Modelling, Ghent University, Coupure links 653, 9000 Gent, Belgium*
[*]*Corresponding author: Tijs W. Alleman, tijs.alleman@ugent.be*

July 17, 2020

## Abstract

As a response to a rapidly rising number of SARS-CoV-2 infections, the Belgian government imposed strict social contact restrictions on March 13th, 2020. After nearly two months, the *curve* was successfully *flattened* and social restrictions were gradually released. Unfortunately, pharmaceutical interventions are not yet available so it is expected that preventing COVID-19 outbreaks will depend mostly on the successful implementation of non-pharmaceutical interventions, hence the need for well-informed models. In this study, we built a deterministic, continuous-time, age-stratified-SEIRD model with detailed hospital dynamics. Because the hospitalization data for Belgium have not been made public yet by the Belgian scientific institute of public health, we computed the hospitalization parameters based on data from 370 patients in two Ghent (Belgium) hospitals. The basic reproduction number during March 2020 was estimated as $R_0 = 2.83$ and the model fits the hospitalization and ICU admission incidence under lockdown measures well. Despite the release of social restrictions, hospitalizations have been steadily declining. We recomputed the basic reproduction number under lockdown release and found that it had to be as low as $R_0 = 0.73$ to explain the endemic trend. We further found that although the basic reproduction number in the population older than 70 years was smaller than one, this group compromises nearly half of the expected hospitalizations. This indicates that the protection of the elderly may be the most efficient way to reduce strain on the public health care system in case of another SARS-CoV-2 outbreak.

**keywords:** epidemiological modeling, SARS-CoV-2, non-pharmaceutical interventions, social contact patterns, hospitalization parameters

# 1 Introduction

After an initial outbreak in early 2020 in Wuhan, China, *Severe acute respiratory syndrome coronavirus 2* (SARS-CoV-2) has spread globally [1]. SARS-CoV-2 is capable of sustained human-to-human transmission [2], and causes severe disease, especially in older individuals. The COVID-19 pandemic has, in general, shown a remarkedly low incidence among children and young adults [3, 4]. Children have a lower susceptibility to infection and a lower propensity to show clinical symptoms [5]. Furthermore, pre-symptomatic transmission is a major contributor to SARS-CoV-2 spread [6, 7]. Unfortunately, pharmaceutical interventions such as vaccination and antiviral drugs are not yet available. On March 13th, 2020, the Belgian government was forced to impose strict social restrictions after tracing methods had failed to prevent large-scale spread of SARS-CoV-2. One and a half months later, the curve was succesfully flattened and social restrictions were gradually relaxed during the months of May, June and the beginning of July. In spite of the relaxations, hospitalizations have kept declining. It is expected that during the coming year(s), preventing COVID-19 outbreaks will depend mostly on the successful implementation of non-pharmaceutical interventions such as social distancing, testing, contact tracing and quarantine. Hence the need for well-informed models that can assist policymakers in choosing the best non-pharmaceutical interventions in case of another large-scale SARS-CoV-2 outbreak. Currently, two other models exist to make predictions for Belgium, the agent-based model of Willem et al. [8] and the discrete-time, stochastic metapopulation model of Coletti et al. [9].

We built a deterministic, continuous-time, age-stratified, extended SEIRD model and calibrated it to overarching Belgian hospitalization data. The model accounts for pre-symptomatic and asymptomatic transmission. Furthermore, the susceptibility to SARS-CoV-2, the severity of the disease and the susceptibility to a subclinical infection depend on the age of the individual. We used social contact rates from a 2008 landmark study by Mossong [10] to model age-specific social mixing. Because detailed hospitalization data have not yet been made publicly available by the Belgian scientific institute of public health (Sciensano), we derived age-stratified hospitalization parameters from data of 370 patients in two Ghent (Belgium) hospitals. In attendence of a more favorable data policy at Sciensano, and thus a more exhaustive dataset, we used the computed hospitalization parameters as temporary proxies to fit the model to the total number of patients in Belgian hospitals and ICU units. Using the model, we computed the basic reproduction number ($R_0$) during the March 2020 epidemic. Because the model systematically overpredicted the hospitalizations during lockdown release, we re-estimated the basic reproduction using data from May 2020 until July 2020.

This paper presents an in-depth study of the effects of non-pharmaceutical measures taken in March 2020 by the Belgian government to prevent SARS-CoV-2 spread. We discuss the large differences in terms of the rate of virus spread and the severity of the disease in individuals of different ages. We further discuss the limitations of our compartmental model to predict COVID-19 outbreaks during the summer of 2020. This work is aimed at informing policymakers to make well-founded decisions in case of future large-scale COVID-19 outbreaks and is aimed at informing the scientific community on the non-pharmaceutical response of the Belgian government to the March, 2020 COVID-19 epidemic.

# 2 Materials and methods

## 2.1 The extended SEIRD-model

### 2.1.1 Model dynamics

The SEIR(D) model was first proposed in 1929 by two Scottish scientists [11]. It is a compartmental model that subdivides the human population into four types of people: 1) susceptible individuals, 2) exposed individuals in the latent phase[1], 3) infectious individuals capable of transmitting the disease and 4) individuals removed from the population either through immunization or death. Despite being a simple and idealized reality, the SEIR(D) dynamics are used extensively to predict the outbreak of infectious diseases and this was no different during the SARS-CoV-2 outbreak earlier this year [12, 1, 5].

In this work, we extend the SEIRD model to incorporate more expert knowledge on SARS-CoV-2. For that purpose, the infectious compartment is split into four parts. The first is a period of pre-symptomatic infectiousness. Several studies have shown that pre-symptomatic transmission is a dominant transmission mechanism of SARS-CoV-2 [7, 6]. After the period of pre-symptomatic transmission, three possible infectious outcomes are modeled: (1) Asymptomatic outcome, for individuals who show no symptoms at all. (2) Mild outcome, for individuals with mild symptoms who recover at home. (3) Hospitalization, when mild symptoms worsen. Children and young adults have a high propensity to experience an asymptomatic or mild outcome, while older individuals have a high propensity to be hospitalized [6, 7].

In general, hospitals have two wards for COVID-19 patients: 1) *Cohort*, where patients are not monitored permanently and 2) *Intensive care*, for patients with the most severe symptoms. Intensive care needs include permanent monitoring, the use of ventilators or the use of ECMO. Patients generally spend limited time in the emergency room and/or in a buffer ward before going to Cohort. After spending limited time in Cohort, some patients are transferred to ICU. Patients can perish in both wards, but mortalities are generally lower in Cohort. After a stay in an ICU, patients return to Cohort for recovery in the hospital. During the recovery stay, mortality is minor. All of the above resulted in a simplified hospital subsystem shown in figure 1.

### 2.1.2 Model framework and equations

In this work, we implemented the extended SEIR dynamics shown in figure 1 using a deterministic approach. The deterministic approach results in a set of N ordinary differential equations, one for every of the 11 population compartments. A deterministic model requires limited computational resources, making it a suitable candidate to rapidly explore scenarios and perform optimizations that require thousands of function evaluations. However, every contact between individuals in the population is assumed to be completely *random*. This simplification is a major limitation of a deterministic implementation. However, we introduced heterogeneity in the deterministic implementation by

[1]The incubation period is composed of two parts, a non-infectious latent period and a period of pre-symptomatic infectiousness.

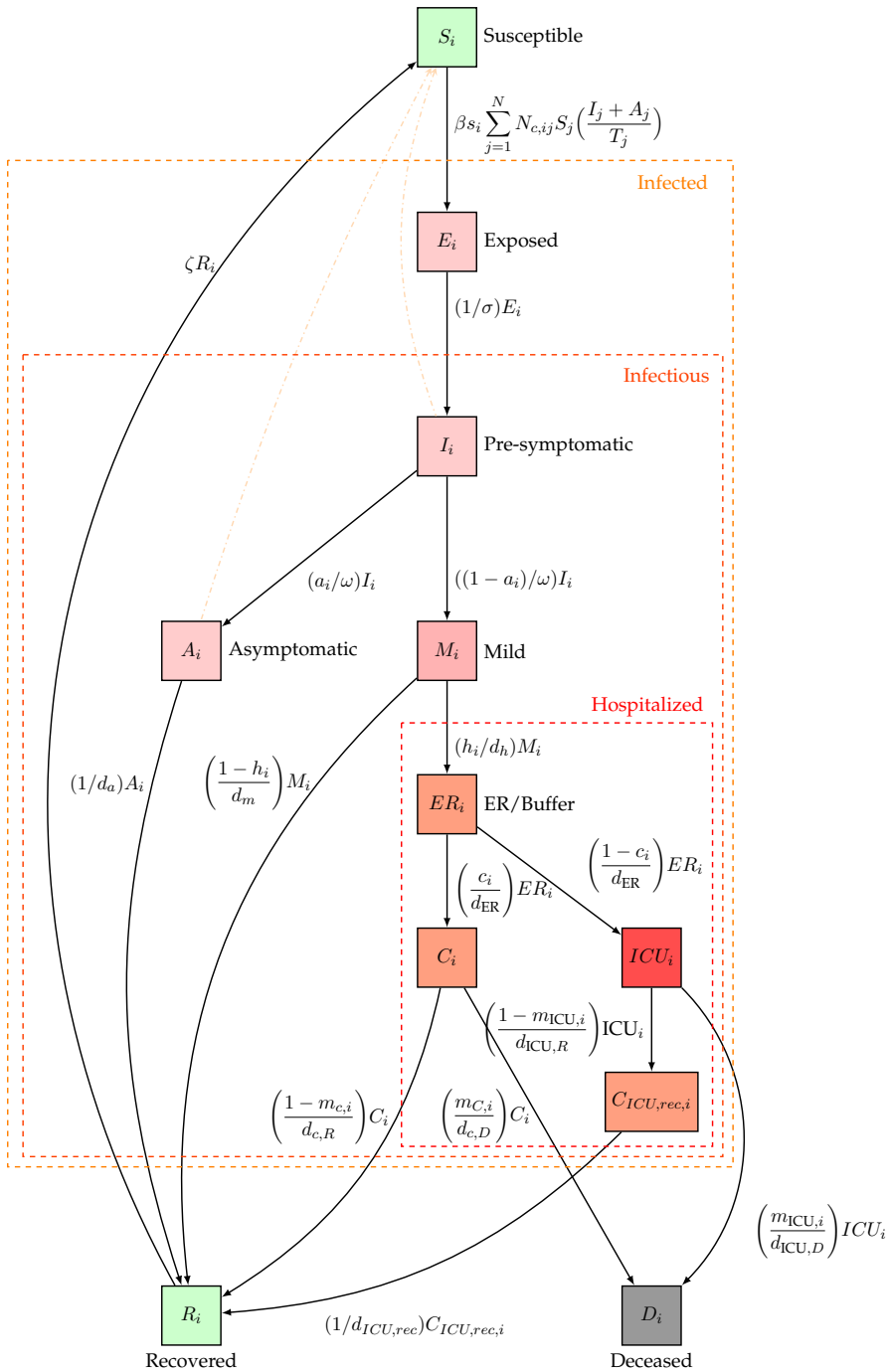


**Figure 1:** Extended SEIRD dynamics used in this study. Nodes represent the model states while edges denote transfers. An overview of the model parameters can be found in table 8.

means of age-stratification. Every population compartment (figure 1) is split into a number of age classes, the age-groups have different contact rates with other age-groups and the disease progresses differently for each age-group, making the model behaviour more realistic. Our age-stratified model consists of 9 age classes, i.e., [0-10), [10-20), [20-30), [30-40), [40-50), [50-60), [60-70), [70-80), [80- $\infty$). The age-stratified deterministic implementation provides a good balance between added complexity and computational resources. The model dynamics are translated into the following system of coupled ordinary differential equations,

$$\dot{S}_i = -\beta s_i \sum_{j=1}^{N} N_{c,ij} S_j \Big(\frac{I_j + A_j}{T_j}\Big) + \zeta R_i, \tag{1}$$

$$\dot{E}_i = \beta s_i \sum_{j=1}^{N} N_{c,ij} S_j \Big(\frac{I_j + A_j}{T_j}\Big) - (1/\sigma) \cdot E_i, \tag{2}$$

$$\dot{I}_i = (1/\sigma)E_i - (1/\omega)I_i, \tag{3}$$

$$\dot{A}_i = (\mathsf{a}_i/\omega)I_i - (1/d_{\mathsf{a}})A_i, \tag{4}$$

$$\dot{M}_i = ((1-\mathsf{a}_i)/\omega)I_i - ((1-h_i)/d_m + h_i/d_{\text{hospital}})M_i, \tag{5}$$

$$\dot{ER}_i = (h_i/d_{\text{hospital}})M_i - (1/d_{\text{ER}})ER_i, \tag{6}$$

$$\dot{C}_i = c_i(1/d_{\text{ER}})ER_i - (m_{C,i}/d_{c,D})C_i - ((1-m_{C,i})/d_{c,R})C_i, \tag{7}$$

$$\dot{ICU}_i = (1-c_i)(1/d_{\text{ER}})ER_i - (m_{ICU,i}/d_{\text{ICU},D})ICU_i \tag{8}$$

$$-((1-m_{ICU,i})/d_{\text{ICU},R})ICU_i, \tag{9}$$

$$\dot{C}_{\text{ICU,rec,i}} = ((1-m_{ICU,i})/d_{\text{ICU},R})ICU_i - (1/d_{\text{ICU,rec}})C_{\text{ICU,rec,i}}, \tag{10}$$

$$\dot{D}_i = (m_{ICU,i}/d_{\text{ICU},D})ICU_i + (m_{C,i}/d_{\text{c},D})C_i, \tag{11}$$

$$\dot{R}_i = (1/d_a)A_i + ((1-h_i)/d_m)M_i + ((1-m_{C,i})/d_{c,R})C_i \tag{12}$$

$$+(1/d_{\text{ICU,rec}})C_{\text{ICU,rec,i}} - \zeta R_i, \tag{13}$$

where $T$ stands for total population, $S$ stands for susceptible, $E$ for exposed, $I$ for pre-symptomatic and infectious, $A$ for asymptomatic and infectious, $M$ for mildly symptomatic and infectious, $ER$ for emergency room and/or buffer ward, $C$ for cohort, $C_{\text{ICU,rec}}$ for a recovery stay in Cohort coming from Intensive Care, $ICU$ for Intensive Care Unit, $H$ for hospitalised, $D$ for dead and $R$ for recovered. Using the above notation, all model states are 9x1 vectors,

$$\boldsymbol{S} = [S_1(t)\ S_2(t)\ \ldots\ S_i(t)]^T,$$

where $S_i(t)$ denotes the number of susceptibles in age-class i at time t after the introduction of the virus in the population. As initial condition, one exposed patient in every age class is used. An overview of all model parameters can be found in table 8.

### 2.1.3 Motivation of model parameters

**Transmission rate and social contact data** The transmission rate of the disease depends on the product of four contributions. The first contribution, $(I + A)/N$, is the fraction of contagious individuals in the population. The second contribution, $\boldsymbol{N}_c$, is the average number of human-to-human interactions per day. The third contribution, $\boldsymbol{s}$, is the relative susceptiblity to SARS-CoV-2 infection and the fourth contribution, $\beta$, is the probability of contracting COVID-19 when encountering a contagious individual under the assumption of 100 % susceptibility to SARS-CoV-2 infection. We assume

that the per contact transmission probability $\beta$ is independent of age and we will infer its distribution by calibrating the model to high-level Belgian hospitalization data. The number of human-human interactions, $\boldsymbol{N}_c$, are both place and age-dependent. These matrices assume the form of a 9x9 *interaction matrix* where an entry X, Y denotes the amount of social contacts age group X has with age group Y per day. These matrices are available for homes, schools, workplaces, in public transport, and leisure activities, from the Polymod study by [10]. In this landmark study, the characteristics of 97,904 contacts with different individuals were recorded during one day, including age, sex, location, duration, frequency, and occurrence of physical contact. The total number of social interactions is given by the sum of the contributions in different places,

$$N_{\text{c, total}} = N_{\text{c, home}} + N_{\text{c, schools}} + N_{\text{c, work}} + N_{\text{c, transport}} + N_{\text{c, leisure}} + N_{\text{c, others}} \tag{14}$$

**Latent period, Pre-symptomatic infectiousness** Estimates for the incubation period range from 3.6 days to 6.4 days, with most estimates close to 5 days. For the average serial interval, the period between the onset of symptoms in the primary case and onset of symptoms in the secondary case, estimates range from 4.0 to 7.5 days [13]. These estimates are of the same order of magnitude, which indicates that pre-symptomatic transmission is a contributor to SARS-Cov-2 spread. If the transmission takes place during the symptomatic period of the primary case, the serial interval is longer than the incubation period. However, this relationship can be reversed when pre-symptomatic transmission takes place. The secondary case may even experience illness onset before onset in their infector, resulting in a negative serial interval. Liu et al. [6] estimated that 23 % of transmissions in Shenzen may have originated from pre-symptomatic infections. Wei et al. [7] investigated all 243 cases of COVID-19 reported in Singapore from January 23–March 16 and identified seven clusters of cases in which presymptomatic transmission is the most likely explanation for the occurrence of secondary cases. They determined that presymptomatic transmission exposure occurred 1-3 days before the source patient developed symptoms. In our model, $\sigma$ denotes the length of the latent, non-infectious period while $\omega$ is the length of the pre-symptomatic infectious period. Based on the results of Wei et al. [7], we assume an average pre-symptomatic infectious period of 2 days. If the incubation period is assumed to last 5.2 days [6], the length of the latent period must be 3.2 days.

**Severity of the disease** The model parameter $\boldsymbol{a}$ is the probability of having a subclinical infection and $\boldsymbol{s}$ is the relative susceptibility to a SARS-CoV-2 infection. Several authors have attempted to estimate the fraction of asymptomatic infections. Li et al. [14] estimated that 86 % of coronavirus infections in the country were "undocumented" in the weeks before the government instituted stringent quarantines . However, this figure includes an unknown number of mildly symptomatic cases and is thus an overestimation of the asymptomatic fraction. In Iceland, citizens were invited for testing regardless of symptoms. Of all people with positive test results, 43 % were asymptomatic [15]. As previously mentioned, there is a strong relationship between the age of the patient and the severity of the disease. Wu et al. [16] estimated the relative fraction of asymptomatic cases per age group from publically available Wuhan data. In this study, the subclinical fractions and relative susceptibility per age group estimated by Davies et al. [5] are used (table 1). $\boldsymbol{h}$ is the fraction of mild cases that require hospitalization. $\boldsymbol{c}$ is the fraction of the hospitalized which remain in Cohort. In this study, we use the age-stratified hospitalization probabilities computed by Verity et al. [3] (table 1). The distributions between Cohort and ICU are computed using data from the Ghent University hospital and AZ Maria Middelares (section 2.2).

**Duration of the infectious period** For asymptomatic and mild cases, the duration of infectiousness is determined by the number of days patients are able to shed viral particles. Mild cases were found to have an earlier viral clearance than severe cases, with 90% of mild patients repeatedly testing negative on RT-PCR by day 10 post-onset. By contrast, all severe cases still tested positive at or beyond day 10 post-onset [17]. Multiple studies have reported that patients have the highest viral load of the coronavirus at the time they are diagnosed, with viral loads declining gradually over time [17, 18, 19, 20]. Lescure et al. [18] determined the viral load of five hospitalized patients over time using RT-PCR. Of the five patients studied, the viral load declined over time, and in all but one of the patients, the viral load dropped below the detection limit within 12 days after symptom onset. To et al. [19] performed an observational cohort study on 23 hospitalized patients and found that salivary viral load was highest during the first week after symptom onset and subsequently declined. Zou et al. [20] found a steep decline in viral load between 6 and 12 days after symptom onset. A comparison of viral load between the symptomatic cases and one laboratory confirmed that asymptomatic cases revealed similar viral loads, indicating that asymptomatic individuals are as infectious as symptomatic patients and implies that the viral load alone is not a clear predictor of disease outcome. Given the evidence presented above, we assume the average duration of infectiousness is 7 days for the symptomatic and asymptomatic cases ($d_a = d_m = 7$ days).

**Hospitalizations** $d_{\text{ER}}$ is the time a patient spends in the emergency room and/or buffer wards before going to Cohort or ICU. $d_{\text{hosp}}$ is the average time between first symptoms and hospitalization, which was previously estimated as 5-9 days by Linton et al. [21] and as 4 days by To et al. [19]. $d_{c,R}$, $d_{c,D}$, $d_{\text{ICU},R}$ and $d_{\text{ICU},D}$ are the average lengths of a hospital stay in Cohort and in an ICU. The subscript $R$ denotes the duration if the patient recovers, while subscript $D$ denotes the duration if the patient perishes. $d_{\text{ICU,rec}}$ is the length of a recovery and observation stay in Cohort after being in ICU. $\boldsymbol{m_C}$ and $\boldsymbol{m}_{\text{ICU}}$ are the mortalities of patients in Cohort and in ICU. Because detailed hospitalization data has not yet been made publicly available by the Belgian scientific institute of public health (Sciensano), all hospitalization parameters are derived from data of 370 patients obtained from two Ghent (Belgium) hospitals. These parameters are used as temporary proxies to fit the model to the total number of patients in Belgian hospitals and ICU until the complete Belgian dataset is made publically available. The methodology of the analysis is presented in section 2.2, the results are presented in section 3.1.

**Testing, tracing and quarantine, re-susceptibility** No testing and tracing are used in this study. The parameter $\zeta$ denotes the fraction of the recovered patients losing immunity and becoming susceptible to SARS-CoV-2 again. Liu et al. [22] found that after SARS-CoV-2 infection, it is unlikely that long-lasting protective antibodies are produced. It is thus deemed likely that re-susceptibility will play an important role in future modeling work. However, at the time of writing, quantitative clinical evidence on re-susceptibility is relatively weak. For now, we thus assume no re-susceptibility of recovered individuals ($\zeta = 0$).

### 2.1.4 Computation of the basic reproduction number

The basic reproduction number $R_0$, defined as the expected number of secondary cases directly generated by one case in a population where all individuals are susceptible to infection, is computed

using the next generation matrix (NGM) approach introducted by [23, 24]. For our model, the basic reproduction number of age group $i$ is,

$$R_{0,i} = (a_i d_a + \omega) * \beta s_i \sum_{j=1}^{N} N_{c,ij} \tag{15}$$

and the total reproduction number is calculated as the weighted average over all age groups using the demographic data in table 1. The algebra is presented in the supplementary materials (section 8).

**Table 1:** Structure of the Belgian population per 10 year intervals [25]. Relative susceptibility to a COVID-19 infection and subclinical fractions per age group as reported by Davies et al. [5]. Hospitalization probability for symptomatic infections per age group in China [3].

| Age group (years) | number of individuals | Relative susceptibility (%) | Subclinical fraction (%) | Hospitalization (%) |
|---|---|---|---|---|
| $[0-10)$ | 1.305.219 | 0.40 | 0.71 | 0.1 |
| $[10-20)$ | 1.298.970 | 0.38 | 0.79 | 0.3 |
| $[20-30)$ | 1.395.385 | 0.79 | 0.73 | 1.2 |
| $[30-40)$ | 1.498.535 | 0.86 | 0.67 | 3.2 |
| $[40-50)$ | 1.524.152 | 0.80 | 0.60 | 4.9 |
| $[50-60)$ | 1.601.891 | 0.82 | 0.51 | 10.2 |
| $[60-70)$ | 1.347.696 | 0.88 | 0.37 | 16.6 |
| $[70-80)$ | 908.725 | 0.74 | 0.31 | 24.3 |
| $[80-\infty)$ | 658.753 | 0.74 | 0.31 | 27.3 |

## 2.2 Analysis of hospital data

The raw datasets consist of 396 patients from two hospitals in Ghent, Belgium[2]. The format of both hospitals data differed, but generally speaking, for every patient the following data were provided: 1) age, 2) sex, 3) hospital admission date, 4) hospital discharge date, 5) date of ICU transfer, 6) date of ICU discharge, 7) outcome (recovered or deceased). The date at which patients first reported having symptoms was exclusive to the Ghent university hospital dataset. The time spent in the emergency room, buffer ward or triage were exclusive to the AZ Maria Middelares dataset. Data from 26 patients had to be excluded from the analysis because one or more entries were missing. Of the remaining 370 patients, 22 patients were discharged from the emergency room and can not be used in the analysis. Thus, in total, data from the remaining 348 patients were used to compute the following hospitalisation parameters: $\boldsymbol{c}$, $d_{c,R}$, $d_{c,D}$, $d_{\text{ICU},R}$ and $d_{\text{ICU},D}$, $d_{\text{ICU,rec}}$, $\boldsymbol{m_C}$ and $\boldsymbol{m}_{\text{ICU}}$. Data on the length of stay in the emergency room or a buffer ward ($d_{\text{ER}}$) was computed solely using data from AZ Maria Middelares. The average time from symptom onset to hospitalisation ($d_{\text{hosp}}$) was

[2]population $\approx$ 250.000 inhabitants.

computed using the Ghent University hospital data. To determine if the duration of a Cohort or ICU stay differs significantly if the patient recovers or dies, two-sided t-tests were used.

## 2.3 SARS-CoV-2 spread in Belgium

### 2.3.1 Global events leading to the Belgian lockdown

We hereby provide a chronological overview of the key events that led to a lockdown in Belgium on March 17th, 2020 (figure 2). The events relevant to the epidemiological modeling of COVID-19 in Belgium are tabulated in table 3. The epicentre of the pandemic was Wuhan, China, where several patients started showing symptoms of pneumonia between December 8th, 2019 and January 2nd, 2020. A cluster of 41 individuals infected by SARS-CoV-2 was retraced to a local Wuhan wet market. The first COVID-19 related death was reported by Chinese officials on January 10th. By January 22nd, 2020, there were over 571 confirmed cases and 17 deaths in the Chinese Hubei province. Around that time, the first clinically confirmed cases outside mainland China were reported. On January 23rd, a quarantine was issued in Wuhan and Huanggang. The next day, two more Hubei cities, Jingzhou and Xiaogan followed.

Belgium closed its Shengen visa application centres in China on January 30th, 2020, and several other European countries quickly followed. Just four days later, the first clinically diagnosed case was reported in Belgium among nine Belgians evacuees from Hubei province, China [26]. Meanwhile, Italy banned all travel to and from China and had declared a state of emergency on January 31st, 2020. In spite of this, the Belgian government imposed no travel restrictions on tourists going to skiing resorts in Northern Italy during spring break, from February 15th until February 23rd, 2020. It has been suggested that the virus started spreading faster in Belgium as a result of spring break. A second infected patient was treated at Antwerp University hospital on February 29th, 2020 [27].

### 2.3.2 Belgian lockdown

By March 2020, COVID-19 was spreading globally and was officially classified as a pandemic by the WHO on March 11, 2020. On the same day, there were two more notable events: 1) the first confirmed COVID-19 death in Belgium[3] [28],. 2) All non-commercial activity except for supermarkets and pharmacies ceased in Italy, essentially placing the entire population in quarantine. In Belgium, a first measure was announced on March 10th, 2020, when the government *recommended* cancelling all events with more than 1000 attendees [29]. The first legally enforceable measures were taken three days later, on Friday, March 13th, 2020 and included a closure of schools, clubs, bars and restaurants and the closure of all non-essential retail. It was further encouraged to work from home if possible [30]. On March 17th, 2020, additional measures were announced: all non-essential travel was prohibited and strict social distancing measures were enforced by police [31, 32, 33]. The Belgian government was at this point still reluctant to use the word *lockdown* and refered to the situation as a *lockdown light*. A final measure was taken on March 20th, 2020, when the Belgian borders were closed. From this point on, the whole country was in a de-facto quarantine.

[3] Later that day two more patients died [28].

### 2.3.3 Belgian lockdown release

On April 7th, 2020, recycling parks were re-opened and on April 18th, 2020 all gardening centres and hardware stores were re-opened. However, strict social restrictions remained in place and it is assumed that the effect on SARS-CoV-2 spread was negligible. The first phase of lockdown release started on May 4th, 2020 when industry, B2B services and non-essential shops were re-opened. Because the number of hospitalizations was further declining, and because of Mother's Day on May 10th, 2020, social restrictions were relaxed. From May 6th, 2020 it was permitted to merge two *social bubbles* on the condition that both *bubbles* consisted of no more than four people. On May 11th, 2020 all retail shops and businesses were re-opened under strict prevention measures. Where possible, working from home remained the norm. On May 18th, 2020, the second phase of lockdown release started. Elementary and secondary schools were re-opened for graduating classes, with a maximum of 10 students per classroom. On the same day, professions which involve the most human contact, for example, hairdressers, could restart if both worker and client wore a face mask. On June 4th, 2020 the third phase of lockdown release started when bars and restaurants could re-open and gatherings of up to 10 persons were allowed. All kindergartens and elementary schools were re-opened without social distancing. Secondary education operated at roughly 50 % of its normal capacity and under strict prevention measures [34].

### 2.3.4 Translation into linear combinations of contact matrices

**Activity reduction during lockdown** The key events highlighted in table 3 must be translated into linear combinations of the aforementioned interaction matrices $N_c$,

$$N_{\text{c, total}} = \Omega \cdot \Big[ N_{\text{c, home}} + N_{\text{c, schools}} + N_{\text{c, work}} + N_{\text{c, transport}} + N_{\text{c, leisure}} + N_{\text{c, others}} \Big], \tag{16}$$

where one extra parameter, $\Omega$, is introduced to model the effect of prevention measures and behavioural changes. For the sake of simplicity, the effect of prevention measures is assumed to be equal in all places. Based on surveys from the Belgian national bank, 28.6 % of all employees was able to work from home, 29.9 % remained in the workplace and 4.4 % worked both from home and in the workplace. 32.4 % were temporary unemployed and 4.8 % were absent [36]. These data are in line with the *Community Mobility Reports* by *Google*, which show a 60 % reduction in workplace mobility (figure 3). From the *Community Mobility Reports* we deduced that public transport mobility was down 70 % during lockdown. Both schools and all forms of leisure activities were closed until May 18th, 2020. During the lockdown, there was a 30 % decrease in grocery related mobility, and attribute these contacts to $N_{\text{c, others}}$. A 30 % increase in residential mobility was observed during the lockdown, however, this can be misleading. It indicates people spent on average 30 % more time at home every day. However, being 30 % longer at home doesn't necessarily mean having 30 % more contacts. We thus used a coefficient of 1.0 for the home interaction matrix $N_{\text{c,home}}$. Note that the coefficients of the interaction matrices are also influenced by *network* effects and may thus not scale linearly with the decrease in the observed mobility. During a strict lockdown where social *bubbles* are the norm, an intra-household contact does not have the same weight as a random, extra-household contact as long as the virus is out of the social *bubble*. However, lowering the fraction of household

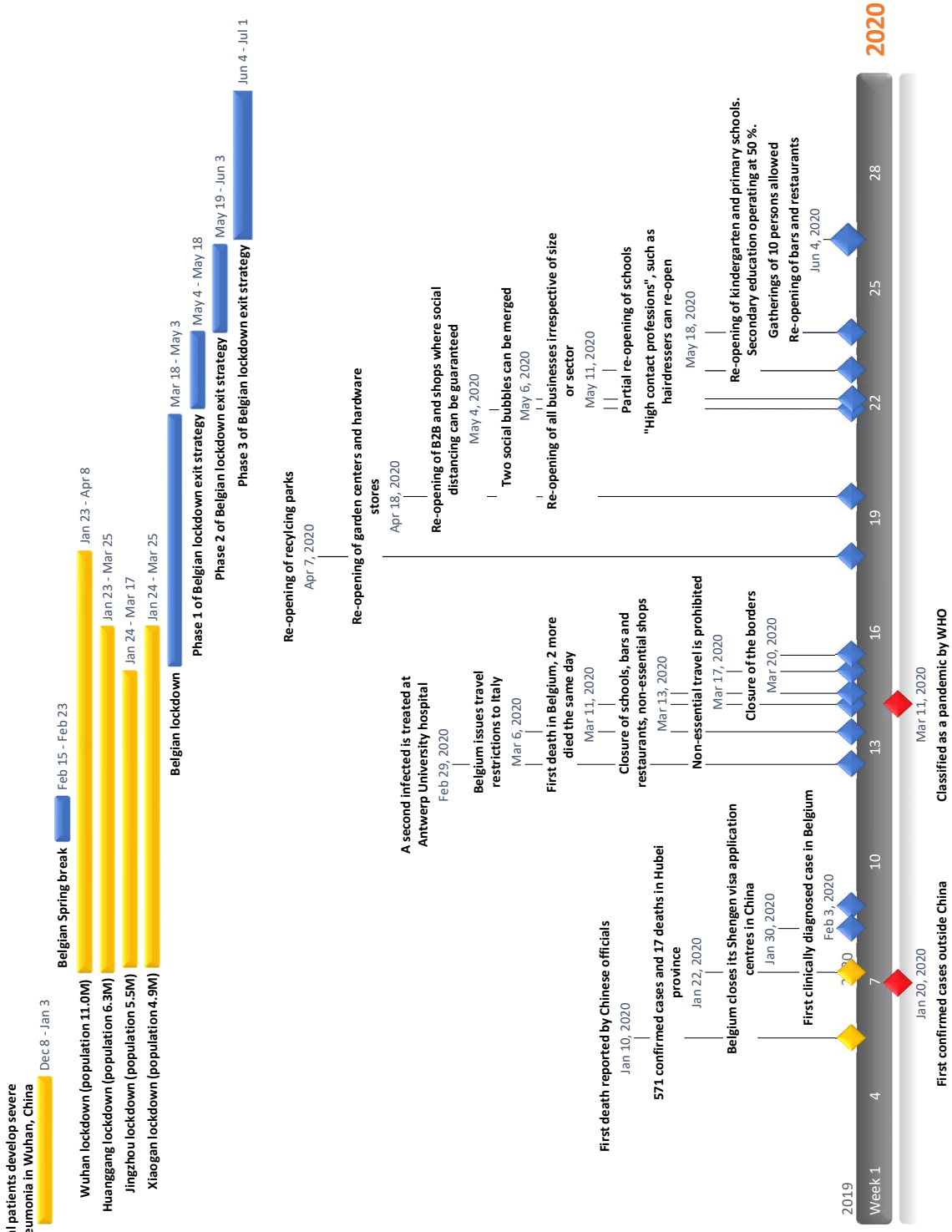


**Figure 2:** Timeline depicting key events during the SARS-CoV-2 pandemic of 2019-2020.

**Table 2:** Key events during the outbreak of the SARS-CoV-2 pandemic in Belgium and during subsequent lockdown release [35, 34].

| Date | Key event | Details |
|---|---|---|
| 13/03/2020 | Lockdown *light* | Closure of schools, bars, clubs and restaurants |
| 17/03/2020 | Lockdown *light* | Closure of all non-essential shops; strict social restrictions enforced by police |
| 20/03/2020 | Border closure | Closure of borders with neighbouring countries. |
| 04/05/2020 | Lockdown release phase Ia | Re-opening of industry and B2B services. Working at home remains the norm where possible. Re-opening of non-essential retail. Face mask obligated on public transport. |
| 06/05/2020 | Lockdown release phase Ia | Merging of two social circles allowed if the second circle consists of no more than 4 people. |
| 11/05/2020 | Lockdown release phase Ib | Re-opening of all businesses and shops, irrespective of size or sector. Strict prevention measures must be respected and working at home remains the norm where possible. |
| 18/05/2020 | Lockdown release phase IIa | Re-opening of schools for graduating classes in elementary and secondary education. Re-opening of businesses which involve the most human-human contact (f.i. hairdressers). |
| 04/06/2020 | Lockdown release phase III | All kindergartens and elementary schools re-opened without social distancing. Secondary education operating at roughly 50 % capactiy. Gatherings up to 10 persons are allowed. Re-opening of bars and restaurants. |
| 01/07/2020 | Lockdown release phase IV | Closure of schools for summer holidays. Re-opening of amusement parks, cinemas and venues (up to 50 persons). Cultural events up to 200 attendees are allowed. Gatherings of up to 15 persons are allowed. |

contacts will drastically reduce mixing of the population and may lead to underestimations of the hospitalizations. Using the above mobility data, the linear combination of interaction matrices used to model government policies from March 17th 2020 until May 4th 2020 is,

$$N_{\text{c, total}} = \Omega \cdot \left[1.0 * N_{\text{c, home}} + 0.4 * N_{\text{c, work}} + 0.3 * N_{\text{c, transport}} + 0.7 * N_{\text{c, others}}\right] \tag{17}$$

**Activity increase during lockdown release** To model the effects of the lockdown release, we derived the coefficients for the workplaces, schools, public transport, leisure and others from the *Google community mobility report* (figure 3). Schools are assumed to operate at only one sixth of their

maximum capacity from May 18th, 2020 until June 4th, 2020[4]. From June 4th, 2020 until July 1st, 2020, all primary schools are open (50.8 % of students) and secondary schools (31.1 % of students) operate at roughly half their usual capacity. Universities (18.1 % of students) remain closed until september.

**Obedience to measures** The model takes into account the effect of *social inertia* when measures are taken. In reality, social restrictions or relaxations represent a change in behaviour which is gradual and cannot be modeled using a step-wise change of the social interaction matrix $N_c$. This effect can be seen upon close inspection of the *Google community mobility report* in figure 3. Multiple functions can be used to model the effects of social compliance, e.g. a delayed or non-delayed ramp, or a logistic function. In our model, we use a delayed ramp to model compliance,

$$N_c^k = N_{\text{c, old}} + f^k * (N_{\text{c, new}} - N_{\text{c, old}}) \tag{18}$$

where,

$$f^k = \begin{cases} 0.0, & \text{if } k \leq \tau \\ \frac{1}{l} * k - \frac{1}{l} * \tau, & \text{if } \tau < k \leq \tau + l \\ 1.0, & \text{otherwise} \end{cases}$$

where $\tau$ is the number of days before measures start having an effect and $l$ is the number of additional days after the time delay until full compliance is reached. Both parameters are calibrated to the hospitalization data. $k$ denotes the number of days since a change in social policy.

**Table 3:** Coefficients used in the linear combinations of social contact matrices ($N_c$) to model the past policies taken by Belgian officials.

| **Date** | $\Omega$ | $\mathbf{N_{c,home}}$ | $\mathbf{N_{c,work}}$ | $\mathbf{N_{c,schools}}$ | $\mathbf{N_{c,transport}}$ | $\mathbf{N_{c,leisure}}$ | $\mathbf{N_{c,others}}$ |
|---|---|---|---|---|---|---|---|
| Lockdown | | | | | | | |
| 13/03/2020 | 1.00 | 1.00 | 1.00 | 1.00 | 1.00 | 1.00 | 1.00 |
| 17/03/2020 | tbd | 1.00 | 0.40 | 0.00 | 0.3 | 0.20 | 0.65 |
| Lockdown release phase I | | | | | | | |
| 04/05/2020 | tbd | 1.00 | 0.50 | 0.00 | 0.40 | 0.30 | 0.70 |
| 06/05/2020 | tbd | 1.00 | 0.60 | 0.00 | 0.45 | 0.35 | 0.75 |
| 11/05/2020 | tbd | 1.00 | 0.70 | 0.00 | 0.50 | 0.40 | 0.80 |
| Lockdown release phase II | | | | | | | |
| 18/05/2020 | tbd | 1.00 | 0.70 | 0.15 | 0.55 | 0.50 | 0.85 |
| Lockdown release phase III | | | | | | | |
| 04/06/2020 | tbd | 1.00 | 0.75 | 0.65 | 0.65 | 0.70 | 0.90 |
| Lockdown release phase IV | | | | | | | |
| 01/07/2020 | tbd | 1.00 | 0.80 | 0.00 | 0.80 | 1.00 | 1.00 |

[4] 2/12 classes are going back to school

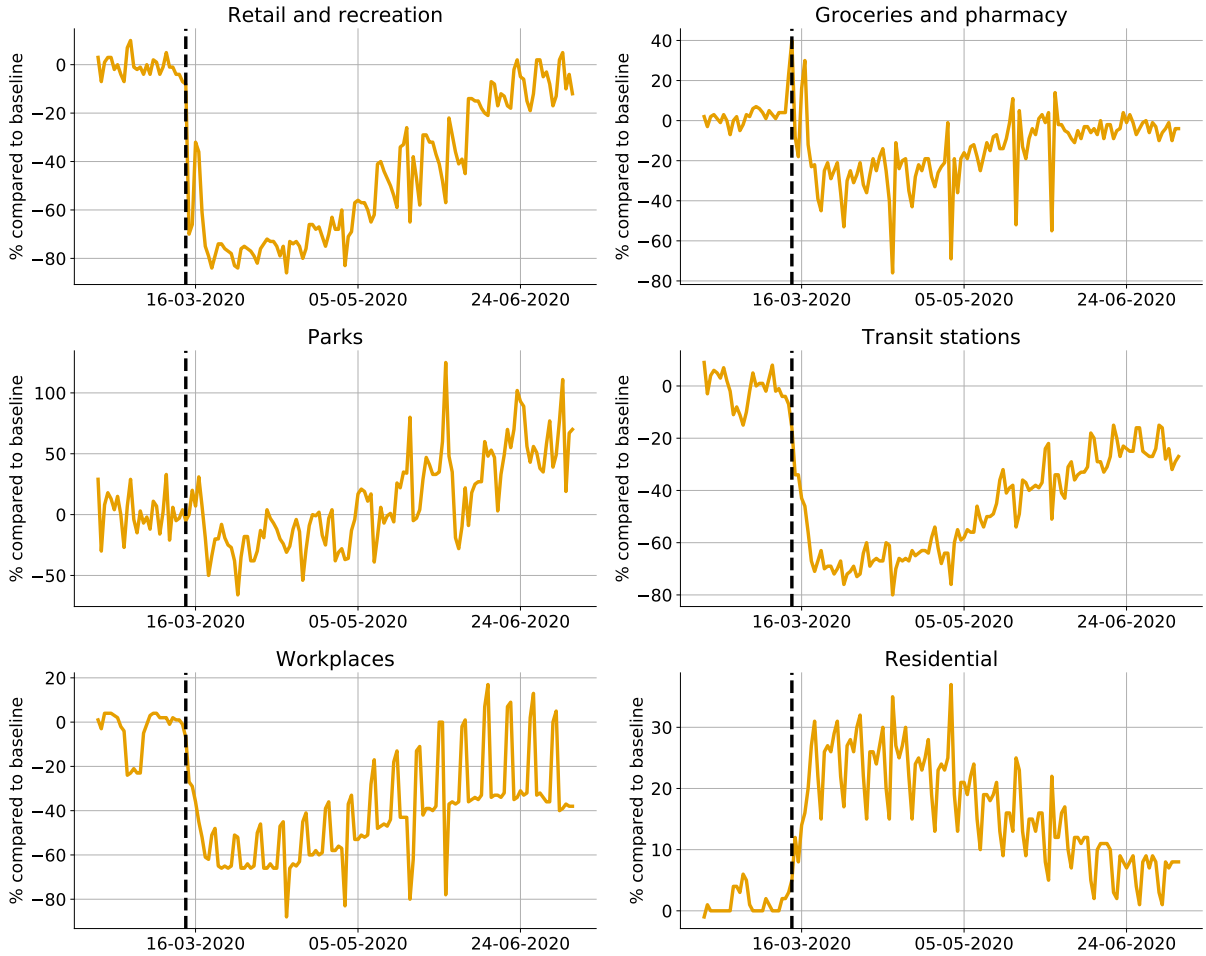


**Figure 3:** Data extracted from the *Google Community Mobility Reports*. Dashed line indicates Friday March 13th, 2020.

## 2.4 Parameter identification and model predictions

Before proposing any scenarios, it is necessary to calibrate the following model parameters to the available hospitalization data: $\beta$, $l$, $\tau$, $\Omega$. The aim of such a calibration is to obtain a parameter distribution which leads to a good agreement between the model predictions and the experimental data. Five timeseries starting on Sunday, March 15th, 2020 have been made publically available by Sciensano,

- the total number of patients in the hospitals ($H_{\text{tot}}$)
- the total number of patients in ICU ($ICU_{\text{tot}}$)
- the daily hospitalizations ($H_{\text{in}}$)
- the daily hospital discharges ($H_{\text{out}}$)
- the daily number of deaths ($D_{\text{new}}$)

We assume that our timeseries are independant and identically distributed (i.d.d.) sequences of normal random variables having a mean $\hat{y}(k)$ and an unknown variance $\hat{\sigma}^2$. The resulting log-likelihood function is,

$$ln\big(P(y \mid \hat{\boldsymbol{\theta}})\big) = -\frac{1}{2}\sum_{k=1}^{N}\left[\frac{\big(y(k) - \hat{y}(k, \hat{\boldsymbol{\theta}})\big)^2}{\hat{\sigma}^2} + \ln(2\pi\hat{\sigma}^2)\right] \tag{19}$$

where $\hat{\boldsymbol{\theta}}$ and $\hat{\sigma}^2$ are computed to maximize the log-likelihood function. The fitting procedure is performed in two steps. First, the transmission parameter $\beta$ (and thus the basic reproduction number, see equation 15) is calibrated using the daily hospitalizations from March 15th, 2020 until March 21st, 2020. These data are used because they do not depend on the durations of the hospitalizations, $d_c$ and $d_{\text{ICU}}$, which are computed from the limited and imperfect hospital dataset. In addition to the calibration of the transmission parameter $\beta$, the amount of time (in days) between the first infectious individuals entering the country and the onset of data collection (March 15th, 2020) must be estimated. The latter is denoted as *excess time*, $t_e$. Second, the daily hospitalizations ($H_{\text{in}}$) from March 15th, 2020 until April 20th, 2020 were used to infer the slope of the compliance ramp ($l$), as well as the effect of prevention measures and *network* effects in the workplace and on public transport ($\Omega$).

We performed the above optimizations in two steps. First, we used a particle swarm optimization (PSO) algorithm to scan the parameter space and find the global maximum likelihood. We then used the obtained maximum-likelihood estimates as initial values for the ensemble sampler for Markov Chain Monte Carlo (MCMC) proposed by Goodman and Weare [37]. For all parameters, uninformative prior distributions were used. The sampler was always run on $2n$ parallel chains, were $n$ was the number of parameters to be sampled from the posterior distributions. For each chain, we drew at least 50-fold more samples than the autocorrelation time. Next, we visualised the samples using the scatterplot matrix proposed by Foreman-Mackey [38], from hereon referred to as *cornerplot*. In these visualizations, each one- and two-dimensional projection of the sample is plotted to reveal correlations. During each step of the optimization procedure, previously sampled parameters were propagated.

## 2.5 Data acquisition

### 2.5.1 Hospital data

The dynamics of the hospital subsystem were obtained by interviewing scientific staff at the Ghent University hospital. A meeting report was sent to prof. Wim Verbeke, MD of AZ Delta in Roeselare, a smaller regional town with 60,000 inhabitants for verification. The Ghent university hospital data were provided to us by professors Pascal Coorevits, Steven Callens and Ernst Rietzschel. The data from AZ Maria Middelares were provided by Leen Van Hoeymissen.

### 2.5.2 Hospitalizations and deaths

The total number of patients in hospitals, the total number of patients in ICU, the daily hospitalizations, the daily hospital discharges and the daily number of deaths were provided by the Belgian scientific institute of public health (Sciensano) and are available for download at `https://epistat.sciensano.be/Data/COVID19BE.xlsx`.

# 3 Results

## 3.1 Parameters governing hospitalisation

The average time from symptom onset to hospitalisation was 5.7 days. The average stay in the emergency room and/or buffer lasted 1.1 days and the average time between admision in Cohort and admission in ICU was 1.4 days. Of the 348 hospitalised patients, 86 patients (24.7 %) required intensive care at some point during their stay and 262 (75.3 %) remained in Cohort. The overall mortality in the hospital is 19.5 %. The mortality in Cohort is slightly lower at 16.8 % and the mortality in ICU is higher at 27.9 %. The average length of the stay in a Cohort ward is 7.7 and the average length of an ICU stay is 12.5 days days (p-value: $6.8 * 10^{-7}$). The average cohort stay was 8.0 days if the patient had recovered and 6.1 days if the patient had died. The difference in hospitalisation lengths is statistically significant with a p-value of $0.022$. Patients who recovered after their ICU stay (9.9 days) had a significantly shorter stay than those who died (19.3 days, p-value: $1.5 * 10^{-3}$). The average length of a post-ICU recovery and observation stay in Cohort was 6.5 days.

The computed age-stratified hospitalization parameters $\boldsymbol{c}$, $\boldsymbol{m}_{\mathrm{C}}$ and $\boldsymbol{m}_{\mathrm{ICU}}$, are listed in table 4. Older individuals (especially ages 60 and upwards) have a much stronger propensity to a severe SARS-CoV-2 infection than children and young adults. From the age-stratified sample sizes, it can be deduced that older individuals have a much higher chance of hospitalization (a quantification was presented by Verity et al. [3], see table 1). No indivuals under 30 years old were in need of intensive care and no individuals under 40 year old have died in the hospital from a SARS-CoV-2 infection in the dataset. Hence, $\boldsymbol{m}_{\mathrm{C}}$ and $\boldsymbol{m}_{\mathrm{ICU}}$ are equal to 0.0 % for individuals under 40 years old. It is expected that the impact of having no deaths below 40 years old will not affect the goodness-of-fit to the Belgian hospitalization data. We do urge readers to use the computed hospitalization parameters with care, especially when analysing aspects where more accurate estimates of the severity of SARS-CoV-2 in the working population is relevant (e.g. to asses the economic impact).

## 3.2 Social compliance

An overview of the estimated parameters is provided in table 5. For every calibration step, the one- and two-dimensional projections of the posterior samples are supplied in the supplementary materials (section 9). On average, the compliance to social measures have a delay of 3.8 days and an additional 5.5 days are needed to reach full social compliance (figure 9). Full compliance was thus reached 9.3 days after measures were taken. A ramp with no delay ($\tau = 0$) was also calibrated but underestimated the peak hospitalizations (figure 4). From figure 4b it can be deduced that the model predicts the daily hospitalisations in Belgium under lockdown measures well. The effect of prevention measures ($\Omega$) was estimated to be 0.28, thus, the actual contact rates were much lower than would be expected when linearily scaling the contact matrices of Mossong et al. [10] with the community mobility figures from Google.

**Table 4:** Computed fraction of hospitalized in need of intensive care ($c$), mortality in Cohort ($m_C$) and mortality in ICU ($m_{ICU}$) per age group for two Belgian hospitals (n = 370). Values in red represent anamolies due to the relatively small sample size.

| Age group (years) | sample size | $c$ (%) | $m_C$ (%) | $m_{ICU}$ (%) |
|---|---|---|---|---|
| $[0-10)$ | 2 | 100.0 | 0.0 | 0.0 |
| $[10-20)$ | 7 | 100.0 | 0.0 | 0.0 |
| $[20-30)$ | 9 | 80.0 | 0.0 | 0.0 |
| $[30-40)$ | 9 | 87.5 | 0.0 | 0.0 |
| $[40-50)$ | 33 | 78.1 | 8.0 | 14.3 |
| $[50-60)$ | 67 | 74.2 | 2.2 | 6.3 |
| $[60-70)$ | 62 | 61.3 | 0.0 | 16.7 |
| $[70-80)$ | 74 | 64.3 | 17.8 | 44.0 |
| $[80-\infty)$ | 107 | 88.2 | 36.7 | 58.3 |
| **Average** | 370 | 75.3 | 16.8 | 27.9 |

**Table 5:** Mean, lower and upper percentile of the model parameters estimated during the calibration procedure.

| Symbol | Parameter | Mean | Percentile 10 | Percentile 90 |
|---|---|---|---|---|
| $t_e$ | excess time | 53 | - | - |
| $\beta$ | probability of infection | 0.0368 | 0.0364 | 0.0372 |
| $R_0$ | basic reproduction number | 2.86 | 2.83 | 2.89 |
| $\tau$ | time delay of compliance ramp | 3.84 | 1.20 | 6.30 |
| $l$ | time after delay needed to reach full compliance | 5.46 | 1.01 | 10.25 |
| $\Omega$ | effect of prevention measures | 0.28 | 0.25 | 0.32 |

## 3.3 Basic reproduction number ($R_0$)

The basic reproduction number during the March 2020 SARS-CoV-2 outbreak was equal to 2.86 (table 5). In table 6, the basic reproduction number $R_0$ is presented per age group. It is clear that the driving force of the pandemic is the working population. If *superspreading* events in elderly homes are not considered, our results suggest ages 70 and upwards can hardly sustain a SARS-CoV-2 pandemic amongst themselves. The main contributor is the large difference in the average number of daily contacts. Despite the low basic reproduction number of the elderly population, 50 % of the hospitalizations are individuals above 70 years old (figure 5).

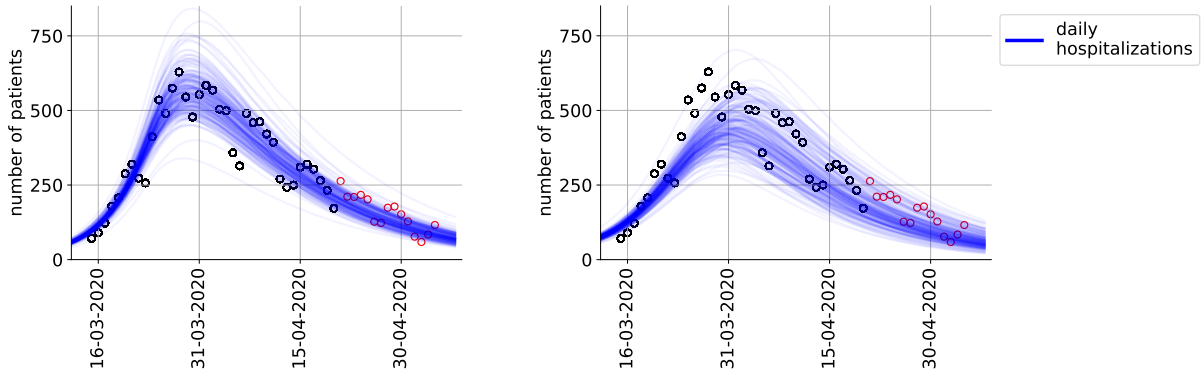


**(a)** Delayed ramp compliance model

**(b)** Ramp compliance model.

**Figure 4:** Model predictions for the daily Belgian hospitalizations during lockdown from March 15th, 2020 until May 5th, 2020. Black markers indicate data were used for the calibration, red markers indicate an extrapolation.

**Table 6:** Average basic reproduction number ($R_{0,i}$) and mean number of daily social contacts per age group ($N_{c,i}$), for Belgium.

| **Age group** | $R_{0,i}$ | **Average** $N_{c,i}$ |
|---|---|---|
| $[0-10)$ | 1.64 | 15.97 |
| $[10-20)$ | 2.01 | 19.06 |
| $[20-30)$ | 4.42 | 21.37 |
| $[30-40)$ | 5.18 | 24.47 |
| $[40-50)$ | 4.07 | 22.31 |
| $[50-60)$ | 2.99 | 17.79 |
| $[60-70)$ | 1.48 | 9.95 |
| $[70-80)$ | 0.84 | 7.37 |
| $[80-\infty)$ | 0.93 | 8.17 |
| **Average:** | 2.83 | 17.34 |

## 3.4 Lockdown release

In figure 6a, the total number of patients in Belgian hospitals and Belgian ICUs are presented together with their respective model prediction. The prediction was made under the assumption that lockdown measures were never released. In spite, the model only slightly underpredicts the hospitalizations. In contrast, if lockdown measures are released on May 4th, 2020 according to the mobility data presented in table 3, a large discrepancy between the model predictions and observations is observed (figure 6b). Post-lockdown, SARS-CoV-2 has thus kept spreading at a rate similar than during the lockdown, in spite of the higher community mobility.

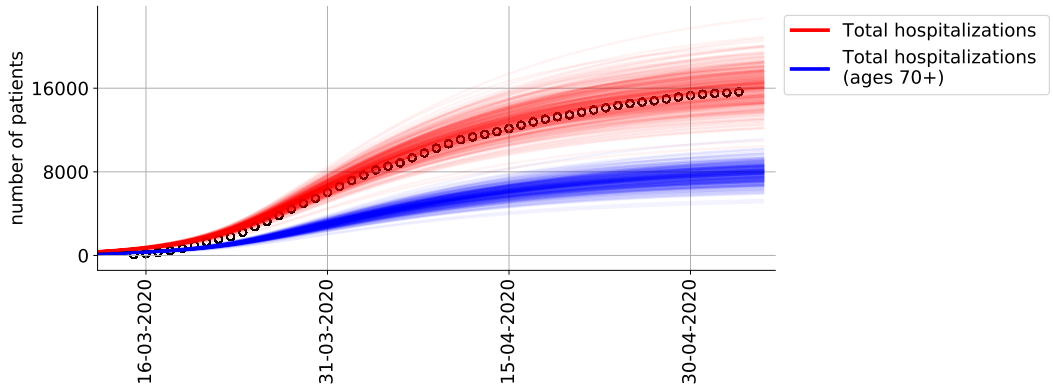


**Figure 5:** Cumulative number of hospitalisations in Belgium from March 15th, 2020 until May 4th, 2020. (red) For all ages. (blue) Ages 70 and above only.

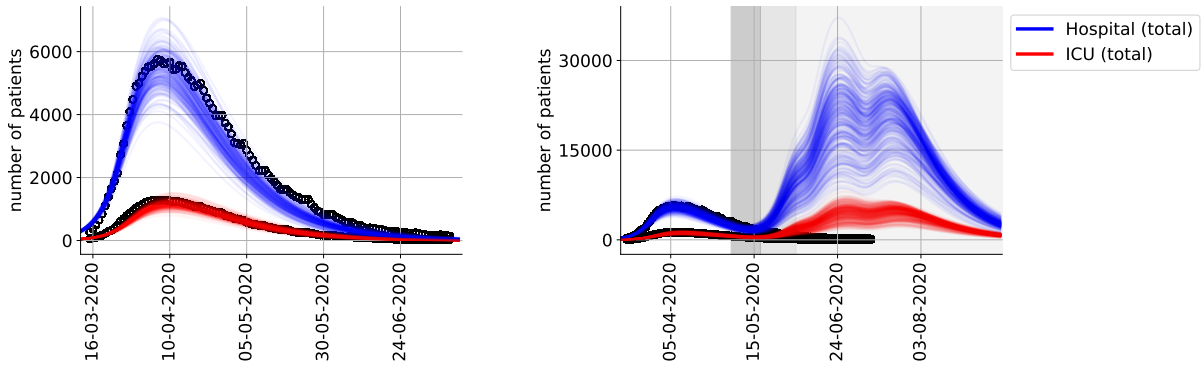


**(a)** Continuation of lockdown.

**(b)** Release of lockdown.

**Figure 6:** Predicted total number of patients in Belgian hospitals (blue) and in Belgian ICUs (red). Shading of the background in figure 6b denotes the phase of lockdown release. From left to right: phase I, II, III (table 3).

## 3.5 Re-estimating the basic reproduction number ($R_0$)

Using the observed hospitalizations from May 5th, 2020 until July 10th, 2020, together with the available google community mobility data the basic reproduction number was re-computed as $R_0 = 0.73$ (table 7). The posterior samples are presented in the supplementary materials (section 9). Altough the population average basic reproduction number is smaller than one, $R_0$ is bigger than one for individuals aged 20 to 50. Because these individuals have a very low propensity of hospitalization, our model predicts that the total number of hospitalizations in Belgium will keep declining during the summer of 2020.

**Table 7:** Apparent basic reproduction number from May 4th, 2020 onwards, per age group ($R_{0,i}$), for Belgium.

| **Age group** | $R_{0,i}$ |
|---|---|
| $[0-10)$ | 0.46 |
| $[10-20)$ | 0.56 |
| $[20-30)$ | 1.23 |
| $[30-40)$ | 1.45 |
| $[40-50)$ | 1.14 |
| $[50-60)$ | 0.83 |
| $[60-70)$ | 0.41 |
| $[70-80)$ | 0.23 |
| $[80-\infty)$ | 0.26 |
| **Average:** | 0.73 |

# 4 Discussion

We computed hospitalization parameters using data from two hospitals in Ghent. The ICU admission probabilities and mortalities in Cohort and in ICU indicate that COVID-19 has a much higher severity in older individuals, which is in line with estimates from authors in the USA and China [40, 3]. The average time from symptom onset to hospitalisation was 5.7 days, which is in line with estimates from Linton et al. [21]. Of the 348 hospitalized patients, 86 patients (24.7 %) required intensive care at some point during their stay and 262 (75.3 %) remained in Cohort. The result is in line with the estimate of Wu and McGoogan [39], who estimated that one quarter of all hospitalized patients requires intensive care. The computed hospitalization parameters are valuable proxies for Belgium and resulted in an adequate goodness-of-fit to the hospitalization and ICU totals under lockdown measures.

We computed the basic reproduction number for Belgium using the daily hospitalizations from March 15th, 2020 until March 21st, 2020. and found that $R_0 = 2.83$, which is in line with the global consensus of $R_0$ in the range 2-3. However, large differences exist between different age groups. It is clear that the working-aged population drive the pandemic (maximum $R_0 = 5.18$) while ages 70 and above can hardly sustain a SARS-CoV-2 pandemic amongst themselves ($R_0 < 1$). In spite, our model indicates that roughly 50 % of all hospitalizations are aged 70 plus. The individuals between 60 and 70 years old should not be neglected, these individuals have a high propensity to hospitalization and generally have more social contact than ages 70 and above. Our model indicates that individuals aged 60 or above account for roughly two thirds of all hospitalizations. These estimates will be refined if the Belgian hospitalization data are made publically available by the scientific institute of public health (Sciensano). *The obtained results indicate that protection of the most vulnerable individuals (elderly) may be an efficient way of reducing strain on the public health system.*

Using the basic reproduction number estimated from the March 2020 hospitalization data, our model

systematically overestimates the current rate of SARS-CoV-2 spread in Belgium. These results indicate that the basic reproduction number obtained by calibration to the hospitalization data from March, 2020, cannot be used to predict SARS-CoV-2 spread from May, 2020 onwards. We re-estimated the basic reproduction number based on the hospitalization data from May- mid July, 2020 , which indicated that the basic reproduction number should have dropped to $R_0 = 0.73$ to model the continued declination in hospitalizations under the observed community mobility. This estimate is in line with the basic reproduction number computed by On Kwok et al. [41] for Hong Kong, Japan and Singapore (0.48-0.70), where SARS-CoV-2 infections have been very local in nature. The authors attributed the small $R_0$ to the early enactment of social distancing interventions and the high level of personal protective measures in these regions. Under the assumption that $R_0 = 0.73$, it is expected that hospitalizations will decline during the summer of 2020 to a baseline of localised infection clusters. These clusters have become too local in nature to use a nation-level deterministic model to make further predictions. This highlights the need to use spatially explicit models. However, if the basic reproduction number re-assumes its March 2020 value of $R_0 = 2.83$ and testing and tracing capacity is insufficient, it is likely that control over SARS-CoV-2 spread will be lost again.

Several factors could have led to a decrease in the basic reproduction number. First, it has been suggested that SARS-CoV-2 is mainly driven by *superspreading events* [42], which are, at the time of writing, still not allowed. Second, from April 6th, 2020 onwards, the weather had improved significantly. No conclusive evidence exists that tropical climates experience slower SARS-CoV-2 spread. However, it has been shown that SARS-CoV-2 can spread through aerosols [43, 44, 45], so poor ventilation of public places contributes to SARS-CoV-2 spread. In Belgium, airconditioning is not customary so public places are now generally well ventilated by opening windows. Third, a mechanism of testing and tracing was implemented in Belgium. However, the efficiency is debatable, as only 13 out of every 40 symptomatic infected individuals provide information [46]. Fourth, the spread of SARS-CoV-2 may not scale linearly with the contributions of each contact matrix $N_c$ as specific behaviours may contribute more to virus spread than others. New contact matrices under lockdown measures were gathered by the Hasselt and Antwerp University SIMID group and will be used in conjunction with our model. An alternative is to determine dominant transmission mechanisms from contact tracing data to further finetune the weights of each contact matrix. Fifth, the COVID-19 epidemic coincided with the annual flu season, which may have reduced the populations resistance to disease. Sixth, some behaviours that promoted SARS-CoV-2 spread, e.g. shaking hands, may have changed permanently.

# 5 Conclusion

- We built a deterministic, continuous-time, age-stratified, extended SEIRD model to investigate the effects of non-pharmaceutical intervention taken by the Belgian government to prevent SARS-CoV-2 spread in March 2020. The model features a detailed representation of hospitals with parameters derived from two Ghent (Belgium) hospitals.
- We estimated the basic reproduction number as $R_0 = 2.83$ during the initial outbreak in March 2020. However, under the release of social restrictions, we computed the basic reproduction

number had to be as low as $R_0 = 0.73$ to explain the endemic trend in the number of hospitalizations, and several plausible explanations were discussed.

- From July 2020, clusters of SARS-CoV-2 infections have become are very local in nature. This makes it hard to present scenarios for the future without making drastic assumptions and highlights the need for spatially explicit models.
- We found that SARS-CoV-2 strongly discriminates between different generations and protection of the elderly may be an efficient way of reducing strain on the public health system. We recommend policymakers to start sensitizing the different generations on their role in SARS-CoV-2 spread. It is detrimental that *children and young adults realize they are a disease vector, much like mosquitos transmitting malaria without suffering its deadly consequences, while older adults must be sensitized to the health risks associated with going to crowded public places unprotected.*

## Acknowledgements

This work is the result of a team effort. I want to thank acknowledge my BIOMATH collegues Bram De Jaegher and Daan Van Hauwermeiren for their help in maintaining the Biomath GitHub repo and coding the visualizations. I want to thank Stijn Van Hoey and Joris Van den Bossche for their help in the coding effort. I would like to thank Mieke Descheppere, statistician at the Ghent university hospital and Wim Verbeke, MD from AZ Delta Roeselare, for sharing their insights on hospital dynamics with me. I would like to thank prof. Steven Callens, MD, prof. Pascal Coorevits, MD and prof. Ernst Nietzschel, MD of the Ghent university hospital and Leen Van Hoeymissen from AZ Maria Middelares for sharing their data with us. The computational resources and services used in this work were provided by the VSC (Flemish Supercomputer Center), funded by the Research Foundation Flanders (FWO) and the Flemish Government – department EWI."

## Competing interests

The authors have no competing interests to declare.

## Role of the funding source

This work was supported by *Bijzonder Onderzoeksfonds UGent* (BOF). The funding source played no role in study design; in the collection, analysis and interpretation of data; in the writing of the report; and in the decision to submit the article for publication.

## CRediT author statement

**Tijs W. Alleman:** Conceptualization, Software, Methodology, Investigation, Data Curation, Writing - Original Draft. **Jenna Vergeynst:** Conceptualization, Software, Writing - Review & Editing, Project administration **Elena Torfs:** Conceptualization, Funding acquisition **Daniel Illana:** Visualization **Ingmar Nopens:** Conceptualization, Funding acquisition, Project administration, Writing - Review &

Editing **Jan Baetens:** Conceptualization, Funding acquisition, Project administration, Writing - Review & Editing

# 6 Model parameters

**Table 8:** Overview of simulation parameters used in the age-stratified extended SEIR model.

| Symbol | Parameter | Value | Unit | Reference |
|---|---|---|---|---|
| $\boldsymbol{a}$ | subclinical fraction | table 1 | $(-)$ | Davies et al. [5] |
| $\boldsymbol{s}$ | relative susceptibility to infection | table 1 | $(-)$ | Davies et al. [5] |
| $\boldsymbol{h}$ | fraction of mildly infected individuals requiring hospitalisation | table 1 | $(-)$ | Verity et al. [3] |
| $\boldsymbol{c}$ | fraction of hospitalisations requiring ICU transfer | table 4 | $(-)$ | Hospital dataset |
| $d_a$ | duration of subclinical infection | 7 | days | To et al. [19] |
| $d_m$ | duration of mild infection | 7 | days | To et al. [19] |
| $d_{\text{hosp}}$ | average time from symptom onset to hospitalization | $\Gamma(1.73,\ 4.36)$ or 5.7 | days | Hospital dataset |
| $d_{\text{ER}}$ | time spent in the emergency room and/or in a buffer ward | 2.5 | days | Hospital dataset |
| $d_{c,R}$ | length of Cohort stay if recovered | 8.0 | days | Hospital dataset |
| $d_{c,D}$ | length of Cohort stay if deceased | 6.1 | days | Hospital dataset |
| $d_{\text{ICU},R}$ | length of ICU stay if recovered | 9.9 | days | Hospital dataset |
| $d_{\text{ICU},D}$ | length of ICU stay if deceased | 19.3 | days | Hospital dataset |
| $d_{\text{ICU,rec}}$ | length of recovery and observation stay in Cohort after ICU stay | 6.5 | days | Hospital dataset |
| $\boldsymbol{m_C}$ | mortality in Cohort | table 4 | $(-)$ | Hospital dataset |
| $\boldsymbol{m_{ICU}}$ | mortality in ICU | table 4 | $(-)$ | Hospital dataset |
| $\sigma$ | length of latent period | 3.2 | days | computed |
| $\omega$ | length of pre-symptomatic infectious period | 2.0 | days | Wei et al. [7] |
| $\sigma + \omega$ | length of incubation period | 5.2 | days | Liu et al. [6] |
| $\beta$ | probability of infection upon contact with an individual capable of transmitting SARS-CoV-2 under the assumption that the infectee is 100 % susceptible to SARS-CoV-2 infection | 0.0368 | $(-)$ | |
| $\boldsymbol{T}_0$ | total population | table 1 | people | Belgian Federal government [25] |
| $N_c$ | contact matrix | 9x9 matrix | day$^{-1}$ | Mossong et al. [10] |
| $\zeta$ | re-susceptibility | 0 | day$^{-1}$ | - |

# 7 Model assumptions

The following assumptions were made to the general extended SEIRD dynamics,

1. All individuals experience a brief pre-symptomatic, infectious period.
2. All ages are assumed equally infectiousness but are not equally susceptible. Children are less susceptible to a SARS-CoV-2 infection [5].
3. Mildly infected and hospitalized individuals cannot infect susceptibles. The model cannot be used to model the effect of transmission to healthcare workers.
4. All deaths come from hospitals, meaning no patients died outside a hospital. Of the 7703 diseased (01/05/2020), 46% died in a hospital while 53% died in an elderly home. All hospital deaths are confirmed Covid-19 cases while only 16% of elderly home deaths were confirmed. When taking the elderly homes out of the model scope, the assumption that deaths only arise in hospitals is valid as only 0.3% died at home and 0.4% died someplace else (`https://www.info-coronavirus.be/nl/news/trends-laatste-dagen-zetten-zich-door/`).
5. Asymptomatic and mild cases automatically lead to recovery and in no case to death.
6. Recovered patients are assumed to be immune, seasonality is deemed out of scope until sufficient quantitative clinical data is available.

The following assumptions to the real-life hospital dynamics reported by Ghent University hospital were made,

1. The Ghent University Hospital has one additional ward named *Midcare*. Because Midcare is not a universal concept, it was merged with the ICU.
2. All patients spend time in the emergency room and/or buffer ward before going to Cohort.
3. All patients going to ICU first spend some time in Cohort.
4. Ventilator or ECMO needs in ICUs are not modeled.
5. Residence times in Cohort and in ICU differ depending on the outcome of the infection (recovered or deceased).
6. All recovered ICU patients spend some additional time in Cohort (recovery and observation stay).

# 8 Basic reproduction number

Since the system is autonomous, the eigenvalues of the Jacobian matrix evaluated at a hyperbolic equilibrium point can be used to determine the nature of that equilibrium. The basic reproduction number ($R_0$) is computed as the spectral radius of the Jacobian matrix at the disease-free equilibrium [23]. Our model has eight infected states: $E, I, A, M, ER, C$, $C_{\text{ICU,rec}}$ and $ICU$ (figure 1). At the disease-free equillibrium, the whole population i This work was supported by s susceptible to the infectious disease, $S_i = T_i$,

$$\boldsymbol{u^*} = (T_i, 0, 0, 0, 0, 0, 0, 0, 0, 0). \tag{20}$$

The Jacobian $\boldsymbol{J}$ is defined as,

$$\boldsymbol{J} = \begin{bmatrix} \frac{\partial f_1}{\partial x_1}\Big|_{\boldsymbol{u^*}} & \cdots & \frac{\partial f_1}{\partial x_n}\Big|_{\boldsymbol{u^*}} \\ \vdots & \ddots & \vdots \\ \frac{\partial f_m}{\partial x_1}\Big|_{\boldsymbol{u^*}} & \cdots & \frac{\partial f_m}{\partial x_n}\Big|_{\boldsymbol{u^*}} \end{bmatrix}, \tag{21}$$

where $n$ and $m$ are equal to the number of infected compartments. Next, the Jacobian is decomposed in the following form,

$$\boldsymbol{J}^* = (\boldsymbol{T} + \boldsymbol{\Sigma})\boldsymbol{J}\ . \tag{22}$$

The matrix $\boldsymbol{T}$ corresponds to all terms that lead to *transmissions* of SARS-CoV-2, while $\boldsymbol{\Sigma}$ corresponds to all terms that lead to *transitions*. For our model,

$$\boldsymbol{T} = \begin{bmatrix} 0 & \beta s_i \sum_{j=1}^{N} N_{c,ij} & \beta s_i \sum_{j=1}^{N} N_{c,ij} & 0 & 0 & 0 & 0 & 0 \\ 0 & 0 & 0 & 0 & 0 & 0 & 0 & 0 \\ \vdots & \vdots & \vdots & \vdots & \vdots & \vdots & \vdots & \vdots \\ 0 & 0 & 0 & 0 & 0 & 0 & 0 & 0 \end{bmatrix}, \tag{23}$$

where an entry $T_{i,j}$ is the rate at which individuals in infected state $j$ gives rise to individuals in infected state $i$. And,

$$\boldsymbol{\Sigma} = \begin{bmatrix} -1/\sigma & 0 & 0 & 0 & 0 & 0 & 0 & 0 \\ 1/\sigma & -1/\omega & 0 & 0 & 0 & 0 & 0 & 0 \\ 0 & a_i/\omega & -1/d_a & 0 & 0 & 0 & 0 & 0 \\ 0 & (1-a_i)/\omega & 0 & -(\frac{1-h_i}{d_m} + \frac{h_i}{d_{\text{hospital}}}) & 0 & 0 & 0 & 0 \\ 0 & 0 & 0 & \frac{h_i}{d_{\text{hospital}}} & -1/d_{\text{ER}} & 0 & 0 & 0 \\ 0 & 0 & 0 & 0 & \frac{c_i}{d_{\text{ER}}} & -\left(\frac{m_{C,i}}{d_{c,D}} + \frac{1-m_{C,i}}{d_{c,R}}\right) & 0 & 0 \\ 0 & 0 & 0 & 0 & \frac{1-c_i}{d_{\text{ER}}} & 0 & -\left(\frac{m_{\text{ICU},i}}{d_{\text{ICU},D}} + \frac{1-m_{\text{ICU},i}}{d_{\text{ICU},R}}\right) & 0 \\ 0 & 0 & 0 & 0 & 0 & 0 & \frac{1-m_{\text{ICU},i}}{d_{\text{ICU},R}} & -\frac{1}{d_{\text{ICU,rec}}} \end{bmatrix}, \tag{24}$$

where an element $\boldsymbol{\Sigma}^{-1}_{i,j}$ is the expected time that an individual who presently has state $j$ will spend in state $i$ during its entire epidemiological *life*. The next generation matrix (NGM) is then calculated as follows,

$$\text{NGM} = -\boldsymbol{T}\boldsymbol{\Sigma}^{-1} \ . \tag{25}$$

The basic reproduction number $R_0$ is defined as the spectral radius[5] $\boldsymbol{\rho}$ of the next generation matrix [23],

$$R_0 = \boldsymbol{\rho}(-\boldsymbol{T}\boldsymbol{\Sigma}^{-1}) \ , \tag{26}$$

for our model,

$$R_{0,i} = (a_i d_a + \omega)\beta s_i \sum_{j=1}^{N} N_{c,ij} \ . \tag{27}$$

[5]Largest absolute eigenvalue.

# 9 Model calibration

## 9.1 SARS-CoV-2 rate of spread

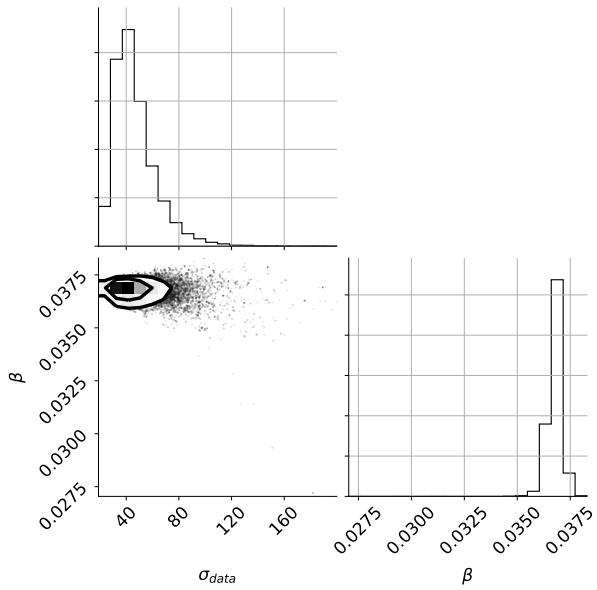


**Figure 7:** One- and two-dimensional projections of the posterior samples for the probability of infection upon contact with an infectious individual ($\beta$) and the uncertainty of the dataset used for the calibration ($\sigma_{\text{data}}$).

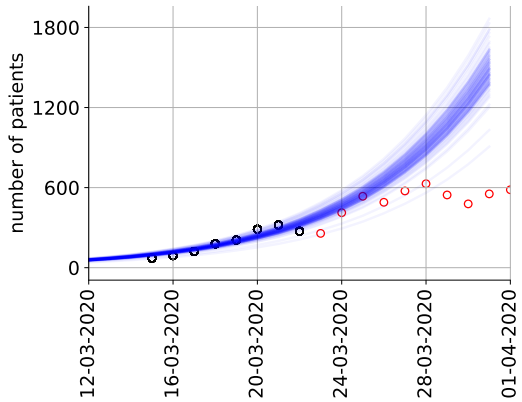


**Figure 8:** Model prediction for the daily Belgian hospitalizations from March 15th, 2020 until April 1st, 2020. Model prediction under the abscense of government measures. Black markers indicate the data were used in the calibration, red markers indicate an extrapolation.

## 9.2 Social compliance and prevention

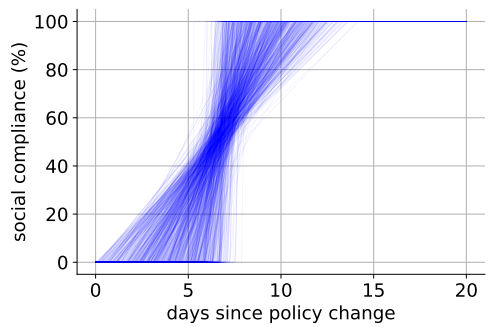


**Figure 9:** Fraction of the population obeying novel social measures in function of the number of days since the policy change. Realisation of 2000 posterior samples of the social compliance delayed ramp.

The delay ($\tau$) and slope ($l$) of the compliance ramp are heavily correlated, however, no correlation between the effect of prevention measures ($\Omega$) and the delay ($\tau$) and slope ($l$) of the ramp parameters was observed (figure 10).

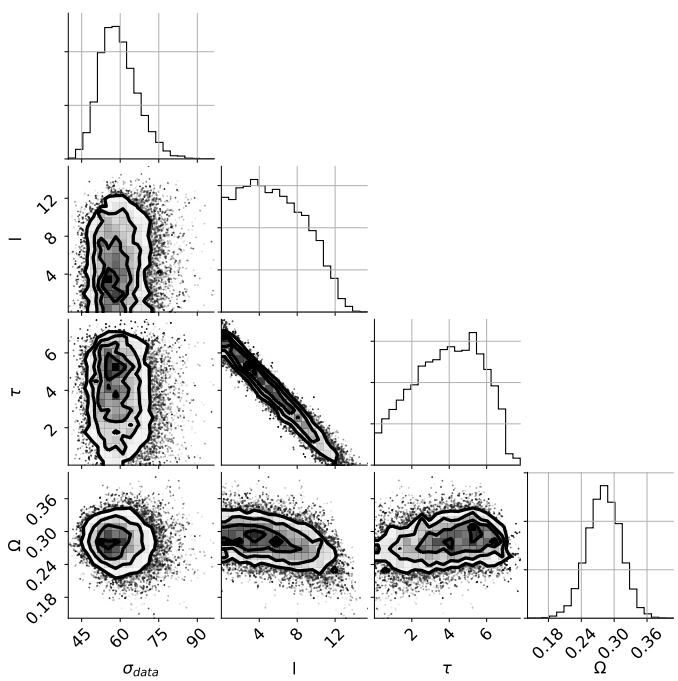


**Figure 10:** One- and two-dimensional projections of the posterior samples for the model parameters that govern social compliance (time-delay, $\tau$ and additional time to reach full compliance, $l$) and the lumped effect of prevention measures and *network effects* ($\Omega$).

## 9.3 Re-estimation of the basic reproduction number

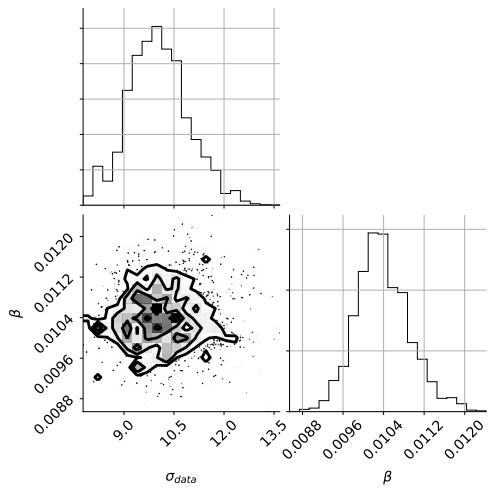


**Figure 11:** One- and two-dimensional projections of the posterior samples for the probability of infection upon contact with an infectious individual ($\beta$) and the uncertainty on the dataset used for the calibration ($\sigma_{\text{data}}$). Mean $\beta$: 0.0104, percentile 10: 0.0097, percentile 90: 0.0111.

# References

[1] Qun Li, Xuhua Guan, Peng Wu, Xiaoye Wang, Lei Zhou, Yeqing Tong, Ruiqi Ren, Kathy S.M. Leung, Eric H.Y. Lau, Jessica Y. Wong, Xuesen Xing, Nijuan Xiang, Yang Wu, Chao Li, Qi Chen, Dan Li, Tian Liu, Jing Zhao, Man Liu, Wenxiao Tu, Chuding Chen, Lianmei Jin, Rui Yang, Qi Wang, Suhua Zhou, Rui Wang, Hui Liu, Yinbo Luo, Yuan Liu, Ge Shao, Huan Li, Zhongfa Tao, Yang Yang, Zhiqiang Deng, Boxi Liu, Zhitao Ma, Yanping Zhang, Guoqing Shi, Tommy T.Y. Lam, Joseph T. Wu, George F. Gao, Benjamin J. Cowling, Bo Yang, Gabriel M. Leung, and Zijian Feng. Early transmission dynamics in wuhan, china, of novel coronavirus–infected pneumonia. *New England Journal of Medicine*, 0(0):null, 2020. doi: 10.1056/NEJMoa2001316. URL `https://doi.org/10.1056/NEJMoa2001316`.

[2] Julien Riou and Christian L. Althaus. Pattern of early human-to-human transmission of wuhan 2019 novel coronavirus (2019-ncov), december 2019 to january 2020. *Eurosurveillance*, 25(4):2000058, 2020. doi: https://doi.org/10.2807/1560-7917.ES.2020.25.4.2000058. URL `https://www.eurosurveillance.org/content/10.2807/1560-7917.ES.2020.25.4.2000058`.

[3] Robert Verity, Lucy C Okell, Ilaria Dorigatti, Peter Winskill, Charles Whittaker, Natsuko Imai, Gina Cuomo-Dannenburg, Hayley Thompson, Patrick G T Walker, Han Fu, Amy Dighe, Jamie T Griffin, Marc Baguelin, Sangeeta Bhatia, Adhiratha Boonyasiri, Anne Cori, Zulma Cucunubá, Rich FitzJohn, Katy Gaythorpe, Will Green, Arran Hamlet, Wes Hinsley, Daniel Laydon, Gemma Nedjati-Gilani, Steven Riley, Sabine van Elsland, Erik Volz, Haowei Wang, Yuanrong Wang, Xiaoyue Xi, Christl A Donnelly, Azra C Ghani, and Neil M Ferguson. Estimates of the severity of coronavirus disease 2019: a model-based analysis. *The Lancet Infectious Diseases*, may 2020. ISSN 1473-3099. doi: 10.1016/S1473-3099(20)30243-7. URL `https://doi.org/10.1016/S1473-3099(20)30243-7`.

[4] Geert Molenberghs, Christel Faes, Jan Aerts, Heidi Theeten, Brecht Devleesschauwer, Natalia Bustos Sierra, Toon Braeye, Francoise Renard, Sereina Herzog, Patrick Lusyne, Johan Van der Heyden, Herman Van Oyen, Pierre Van Damme, and Niel Hens. Belgian covid-19 mortality, excess deaths, number of deaths per million, and infection fatality rates (8 march - 9 may 2020). *medRxiv*, 2020. doi: 10.1101/2020.06.20.20136234. URL `https://www.medrxiv.org/content/early/2020/06/20/2020.06.20.20136234`.

[5] Nicholas G Davies, Adam J Kucharski, Rosalind M Eggo, Amy Gimma, , and W. John Edmunds. The effect of non-pharmaceutical interventions on covid-19 cases, deaths and demand for hospital services in the uk: a modelling study. *medRxiv*, 2020. doi: 10.1101/2020.04.01.20049908. URL `https://www.medrxiv.org/content/early/2020/04/06/2020.04.01.20049908`.

[6] Y Liu, null null, S Funk, and S Flasche. The contribution of pre-symptomatic infection to the transmission dynamics of covid-2019 [version 1; peer review: 1 approved]. *Wellcome Open Research*, 5(58), 2020. doi: 10.12688/wellcomeopenres.15788.1.

[7] Wycliffe E. Wei, Zongbin Li, Calvin J. Chiew, Sarah E. Yong, Matthias P. Toh, and Vernon J. Lee. Presymptomatic Transmission of SARS-CoV-2 — Singapore, January 23–March 16, 2020. *Mor-*

*bidity and Mortality Weekly Report*, 69:411–415, 2020. doi: http://dx.doi.org/10.15585/mmwr.mm6914e1.

[8] Lander Willem, Thang Van Hoang, Sebastian Funk, Pietro Coletti, Philippe Beutels, and Niel Hens. Socrates: An online tool leveraging a social contact data sharing initiative to assess mitigation strategies for covid-19. *medRxiv*, 2020. doi: 10.1101/2020.03.03.20030627. URL `https://www.medrxiv.org/content/early/2020/03/19/2020.03.03.20030627`.

[9] Pietro Coletti, Pieter Libin, Oana Petrof, Steven Abrams, Christel Faes, Elise Kuylen, James Wambua, Lander Willem, Beutels Philippe, and Niel Hens. Covid-19 report on a meta-population model for belgium: a first status report. May 2020. URL `https://www.uhasselt.be/Images/DSI/report_meta.pdf`.

[10] Joël Mossong, Niel Hens, Mark Jit, Philippe Beutels, Kari Auranen, Rafael Mikolajczyk, Marco Massari, Stefania Salmaso, Gianpaolo Scalia Tomba, Jacco Wallinga, Janneke Heijne, Malgorzata Sadkowska-Todys, Magdalena Rosinska, and W. John Edmunds. Social contacts and mixing patterns relevant to the spread of infectious diseases. *PLOS Medicine*, 5(3):1–1, 03 2008. doi: 10.1371/journal.pmed.0050074. URL `https://doi.org/10.1371/journal.pmed.0050074`.

[11] William Ogilvy Kermack, A. G. McKendrick, and Gilbert Thomas Walker. A contribution to the mathematical theory of epidemics. *Proceedings of the Royal Society of London. Series A, Containing Papers of a Mathematical and Physical Character*, 115(772):700–721, 1927. doi: 10.1098/rspa.1927.0118. URL `https://royalsocietypublishing.org/doi/abs/10.1098/rspa.1927.0118`.

[12] Joseph T Wu, Kathy Leung, and Gabriel M Leung. Nowcasting and forecasting the potential domestic and international spread of the 2019-ncov outbreak originating in wuhan, china: a modelling study. *The Lancet*, 395(10225):689 – 697, 2020. ISSN 0140-6736. doi: https://doi.org/10.1016/S0140-6736(20)30260-9. URL `http://www.sciencedirect.com/science/article/pii/S0140673620302609`.

[13] Minah Park, Alex R Cook, Jue Tao Lim, Yinxiaohe Sun, and Borame L Dickens. A Systematic Review of COVID-19 Epidemiology Based on Current Evidence. *Journal of clinical medicine*, 9(4), mar 2020. ISSN 2077-0383 (Print). doi: 10.3390/jcm9040967.

[14] Ruiyun Li, Sen Pei, Bin Chen, Yimeng Song, Tao Zhang, Wan Yang, and Jeffrey Shaman. Substantial undocumented infection facilitates the rapid dissemination of novel coronavirus (sars-cov2). *Science*, 2020. ISSN 0036-8075. doi: 10.1126/science.abb3221. URL `https://science.sciencemag.org/content/early/2020/03/13/science.abb3221`.

[15] Daniel F. Gudbjartsson, Agnar Helgason, Hakon Jonsson, Olafur T. Magnusson, Pall Melsted, Gudmundur L. Norddahl, Jona Saemundsdottir, Asgeir Sigurdsson, Patrick Sulem, Arna B. Agustsdottir, Berglind Eiriksdottir, Run Fridriksdottir, Elisabet E. Gardarsdottir, Gudmundur Georgsson, Olafia S. Gretarsdottir, Kjartan R. Gudmundsson, Thora R. Gunnarsdottir, Arnaldur Gylfason, Hilma Holm, Brynjar O. Jensson, Aslaug Jonasdottir, Frosti Jonsson, Kamilla S. Josefsdottir, Thordur Kristjansson, Droplaug N. Magnusdottir, Louise le Roux, Gudrun Sigmundsdottir, Gardar Sveinbjornsson, Kristin E. Sveinsdottir, Maney Sveinsdottir, Emil A. Thorarensen,

Bjarni Thorbjornsson, Arthur Löve, Gisli Masson, Ingileif Jonsdottir, Alma D. Möller, Thorolfur Gudnason, Karl G. Kristinsson, Unnur Thorsteinsdottir, and Kari Stefansson. Spread of sars-cov-2 in the icelandic population. *New England Journal of Medicine*, 0(0):null, 2020. doi: 10.1056/NEJMoa2006100. URL `https://doi.org/10.1056/NEJMoa2006100`.

[16] Joseph T Wu, Kathy Leung, Mary Bushman, Nishant Kishore, Rene Niehus, Pablo M de Salazar, Benjamin J Cowling, Marc Lipsitch, and Gabriel M Leung. Estimating clinical severity of COVID-19 from the transmission dynamics in Wuhan, China. *Nature Medicine*, 26(4):506–510, 2020. ISSN 1546-170X. doi: 10.1038/s41591-020-0822-7. URL `https://doi.org/10.1038/s41591-020-0822-7`.

[17] Yang Liu, Li-Meng Yan, Lagen Wan, Tian-Xin Xiang, Aiping Le, Jia-Ming Liu, Malik Peiris, Leo L M Poon, and Wei Zhang. Viral dynamics in mild and severe cases of COVID-19. *The Lancet Infectious Diseases*, 0(0), 2020. ISSN 1473-3099. doi: 10.1016/S1473-3099(20)30232-2.

[18] Francois-Xavier Lescure, Lila Bouadma, Duc Nguyen, Marion Parisey, Paul-Henri Wicky, Sylvie Behillil, Alexandre Gaymard, Maude Bouscambert-Duchamp, Flora Donati, Quentin Le Hingrat, Vincent Enouf, Nadhira Houhou-Fidouh, Martine Valette, Alexandra Mailles, Jean-Christophe Lucet, France Mentre, Xavier Duval, Diane Descamps, Denis Malvy, Jean-François Timsit, Bruno Lina, Sylvie Van-der Werf, and Yazdan Yazdanpanah. Clinical and virological data of the first cases of COVID-19 in Europe: a case series. *The Lancet Infectious Diseases*, 0(0), 2020. ISSN 1473-3099. doi: 10.1016/S1473-3099(20)30200-0.

[19] Kelvin Kai-Wang To, Owen Tak-Yin Tsang, Wai-Shing Leung, Anthony Raymond Tam, Tak-Chiu Wu, David Christopher Lung, Cyril Chik-Yan Yip, Jian-Piao Cai, Jacky Man-Chun Chan, Thomas Shiu-Hong Chik, Daphne Pui-Ling Lau, Chris Yau-Chung Choi, Lin-Lei Chen, Wan-Mui Chan, Kwok-Hung Chan, Jonathan Daniel Ip, Anthony Chin-Ki Ng, Rosana Wing-Shan Poon, Cui-Ting Luo, Vincent Chi-Chung Cheng, Jasper Fuk-Woo Chan, Ivan Fan-Ngai Hung, Zhiwei Chen, Honglin Chen, and Kwok-Yung Yuen. Temporal profiles of viral load in posterior oropharyngeal saliva samples and serum antibody responses during infection by SARS-CoV-2: an observational cohort study. *The Lancet Infectious Diseases*, 20(5):565–574, may 2020. ISSN 1473-3099. doi: 10.1016/S1473-3099(20)30196-1. URL `https://www.thelancet.com/journals/laninf/article/PIIS1473-3099(20)30196-1/fulltext{#}.XsE5ulFU1n8.mendeley`.

[20] Lirong Zou, Feng Ruan, Mingxing Huang, Lijun Liang, Huitao Huang, Zhongsi Hong, Jianxiang Yu, Min Kang, Yingchao Song, Jinyu Xia, Qianfang Guo, Tie Song, Jianfeng He, Hui-Ling Yen, Malik Peiris, and Jie Wu. Sars-cov-2 viral load in upper respiratory specimens of infected patients. *New England Journal of Medicine*, 382(12):1177–1179, 2020. doi: 10.1056/NEJMc2001737. URL `https://doi.org/10.1056/NEJMc2001737`. PMID: 32074444.

[21] Natalie M Linton, Tetsuro Kobayashi, Yichi Yang, Katsuma Hayashi, Andrei R Akhmetzhanov, Sung-Mok Jung, Baoyin Yuan, Ryo Kinoshita, and Hiroshi Nishiura. Incubation Period and Other Epidemiological Characteristics of 2019 Novel Coronavirus Infections with Right Truncation: A Statistical Analysis of Publicly Available Case Data. *Journal of clinical medicine*, 9(2), feb 2020. ISSN 2077-0383 (Print). doi: 10.3390/jcm9020538.

[22] Tao Liu, Sanyun Wu, Huangheng Tao, Guang Zeng, Fuling Zhou, Fangjian Guo, and Xinghuan Wang. Prevalence of igg antibodies to sars-cov-2 in wuhan - implications for the ability to produce long-lasting protective antibodies against sars-cov-2. *medRxiv*, 2020. doi: 10.1101/2020.06.13.20130252.

[23] O Diekmann, J.A.P. Heesterbeek, and Metz J.A.J. On the definition and the computation of the basic reproduction ratio R0 in models for infectious diseases in heterogeneous populations. *Journal of mathematical biology*, 28(4):365–382, 1990. ISSN 0303-6812 (Print). doi: 10.1007/BF00178324.

[24] O Diekmann, J.A.P. Heesterbeek, and Roberts M.G. The construction of next-generation matrices for compartmental epidemic models. *Journal of the Royal Society, Interface*, 7(47):873–885, jun 2010. ISSN 1742-5662. doi: 10.1098/rsif.2009.0386. URL `https://pubmed.ncbi.nlm.nih.gov/19892718https://www.ncbi.nlm.nih.gov/pmc/articles/PMC2871801/`.

[25] Belgian Federal government. StatBEL - Structure of the Population, 2020. URL `https://statbel.fgov.be/en/themes/population/structure-population{#}panel-11`.

[26] Dirk Hendrikx. Een vreugdedansje voor de eerste coronapatiënt. *de Standaard*, Mar 2020. URL `https://www.standaard.be/cnt/dmf20200228_04869102`.

[27] Eveline Vergauwen and Marie Garré. Wat weten we over de tweede coronapatiënt in ons land? *de Standaard*, Mar 2020. URL `https://www.standaard.be/cnt/dmf20200301_04870845`.

[28] Drie doden in belgië. *de Standaard*, Mar 2020. URL `https://www.standaard.be/cnt/dmf20200311_04886060`.

[29] Waarom de regering de limiet op duizend mensen legt. *de Standaard*, Mar 2020. URL `https://www.standaard.be/cnt/dmf20200310_04884011`.

[30] Overzicht. dit zijn de nieuwe coronamaatregelen in ons land. *de Standaard*, Mar 2020. URL `https://www.standaard.be/cnt/dmf20200313_04888179`.

[31] Jeffery Dujardin. Daar zijn de eerste coronaboetes: zelfs agenten bespuwd in gent. *de Standaard*, Mar 2020. URL `https://www.standaard.be/cnt/dmf20200320_04897389`.

[32] Emma Verhoeven. Lokale politie zet 10.000 agenten in op naleving coronamaatregelen. *de Standaard*, Mar 2020. URL `https://www.standaard.be/cnt/dmf20200319_04895634`.

[33] Emma Verhoeven. Dit zijn de verstrengde maatregelen in de strijd tegen nieuw coronavirus. *de Standaard*, Mar 2020. URL `https://www.standaard.be/cnt/dmf20200317_04892894`.

[34] Vlaamse regering. Heropstart van de lessen op school: wie, waarom en hoe, 2020. URL `https://onderwijs.vlaanderen.be/nl/heropstart-lessen-op-school-wie-waarom-hoe`.

[35] Open VLD. Coronavirus : België heeft z'n exitstrategie vastgelegd, 2020. URL `https://www2.openvld.be/coronavirus-belgie-heeft-zn-exitstrategie-vastgelegd/`.

[36] Sven Whatty. Tijdelijke werkloosheid bijna gehalveerd. *Het Laatste Nieuws*, June 2020. URL https://www.hln.be/de-krant/tijdelijke-werkloosheid-bijna-gehalveerd~a092a080/?referer=https%3A%2F%2Fwww.google.be%2F.

[37] Jonathan Goodman and Jonathan Weare. Ensemble samplers with affine invariance. *Communications in Applied Mathematics and Computational Science*, 5(1):65–80, January 2010. doi: 10.2140/camcos.2010.5.65.

[38] Daniel Foreman-Mackey. corner.py: Scatterplot matrices in python. *The Journal of Open Source Software*, 1(2):24, jun 2016. doi: 10.21105/joss.00024. URL https://doi.org/10.21105/joss.00024.

[39] Zunyou Wu and Jennifer M. McGoogan. Characteristics of and important lessons from the coronavirus disease 2019 (covid-19) outbreak in china: Summary of a report of 72314 cases from the chinese center for disease control and prevention. *JAMA*, 02 2020. ISSN 0098-7484. doi: 10.1001/jama.2020.2648.

[40] CDC COVID-19 Response Team. Severe Outcomes Among Patients with Coronavirus Disease 2019 (COVID-19) - United States, February 12-March 16, 2020. *Morbidity and Mortality Weekly Report*, 69:343–346, 2020. doi: http://dx.doi.org/10.15585/mmwr.mm6912e2.

[41] Kin On Kwok, Henry Ho Hin Chan, Ying Huang, David Shu Cheong Hui, Paul Anantharajah Tambyah, Wan In Wei, Patsy Yuen Kwan Chau, Samuel Yeung Shan Wong, and Julian Wei Tze Tang. Inferring super-spreading from transmission clusters of COVID-19 in Hong Kong, Japan and Singapore. *The Journal of hospital infection*, pages S0195–6701(20)30258–9, may 2020. ISSN 1532-2939. doi: 10.1016/j.jhin.2020.05.027. URL https://pubmed.ncbi.nlm.nih.gov/32446721https://www.ncbi.nlm.nih.gov/pmc/articles/PMC7242928/.

[42] Dillion Adan, Peng Wu, Jessica Wong, Eric Lau, Tim Tsang, Simon Cauchemez, Gabriel Leung, and Benjamin Cowling. Clustering and superspreading potential of severe acute respiratory syndrome coronavirus 2 (SARS-CoV-2) infections in Hong Kong. *Research Square PREPRINT*, 2020. doi: 10.21203/rs.3.rs-29548/v1.

[43] Rajat Mittal, Rui Ni, and Jung-Hee Seo. The flow physics of covid-19. *Journal of Fluid Mechanics*, 894:F2, 2020. doi: 10.1017/jfm.2020.330.

[44] Lydia Bourouiba. Turbulent Gas Clouds and Respiratory Pathogen Emissions: Potential Implications for Reducing Transmission of COVID-19. *JAMA*, mar 2020. ISSN 1538-3598 (Electronic). doi: 10.1001/jama.2020.4756.

[45] Sima Asadi, Nicole Bouvier, Anthony S Wexler, and William D Ristenpart. The coronavirus pandemic and aerosols: Does COVID-19 transmit via expiratory particles? *Aerosol science and technology : the journal of the American Association for Aerosol Research*, 0(0):1–4, apr 2020. ISSN 0278-6826. doi: 10.1080/02786826.2020.1749229. URL https://pubmed.ncbi.nlm.nih.gov/32308568https://www.ncbi.nlm.nih.gov/pmc/articles/PMC7157964/.

[46] Dries De Smet and Nikolas Vanhecke. Elf contacten? computer says no. *de Standaard*, June 2020. URL https://www.standaard.be/cnt/dmf20200629_05004161.

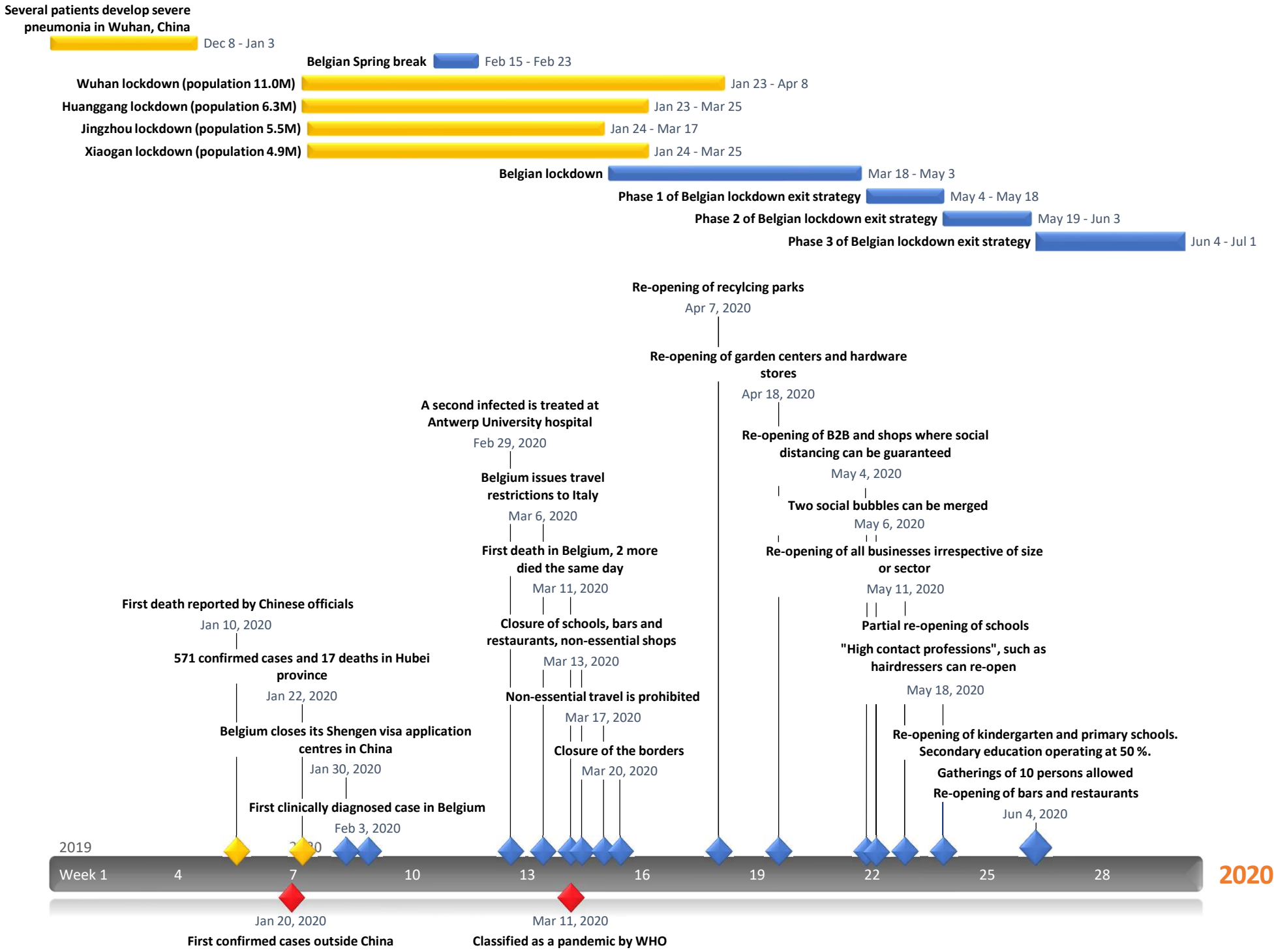
Several patients develop severe pneumonia in Wuhan, China
Dec 8 - Jan 3
Belgian Spring break
Feb 15 - Feb 23
Wuhan lockdown (population 11.0M)
Jan 23 - Apr 8
Huanggang lockdown (population 6.3M)
Jan 23 - Mar 25
Jingzhou lockdown (population 5.5M)
Jan 24 - Mar 17
Xiaogan lockdown (population 4.9M)
Jan 24 - Mar 25
Belgian lockdown
Mar 18 - May 3
Phase 1 of Belgian lockdown exit strategy
May 4 - May 18
Phase 2 of Belgian lockdown exit strategy
May 19 - Jun 3
Phase 3 of Belgian lockdown exit strategy
Jun 4 - Jul 1
Re-opening of recylcing parks
Apr 7, 2020
Re-opening of garden centers and hardware stores
Apr 18, 2020
A second infected is treated at Antwerp University hospital
Feb 29, 2020
Re-opening of B2B and shops where social distancing can be guaranteed
May 4, 2020
Belgium issues travel restrictions to Italy
Mar 6, 2020
Two social bubbles can be merged
May 6, 2020
First death in Belgium, 2 more died the same day
Mar 11, 2020
Re-opening of all businesses irrespective of size or sector
May 11, 2020
First death reported by Chinese officials
Jan 10, 2020
Closure of schools, bars and restaurants, non-essential shops
Mar 13, 2020
Partial re-opening of schools
"High contact professions", such as hairdressers can re-open
May 18, 2020
571 confirmed cases and 17 deaths in Hubei province
Jan 22, 2020
Non-essential travel is prohibited
Mar 17, 2020
Belgium closes its Shengen visa application centres in China
Jan 30, 2020
Closure of the borders
Mar 20, 2020
Re-opening of kindergarten and primary schools. Secondary education operating at 50 %.
Gatherings of 10 persons allowed
Re-opening of bars and restaurants
Jun 4, 2020
First clinically diagnosed case in Belgium
Feb 3, 2020
2019
Week 1
4
7
10
13
16
19
22
25
28
2020
Jan 20, 2020
First confirmed cases outside China
Mar 11, 2020
Classified as a pandemic by WHO

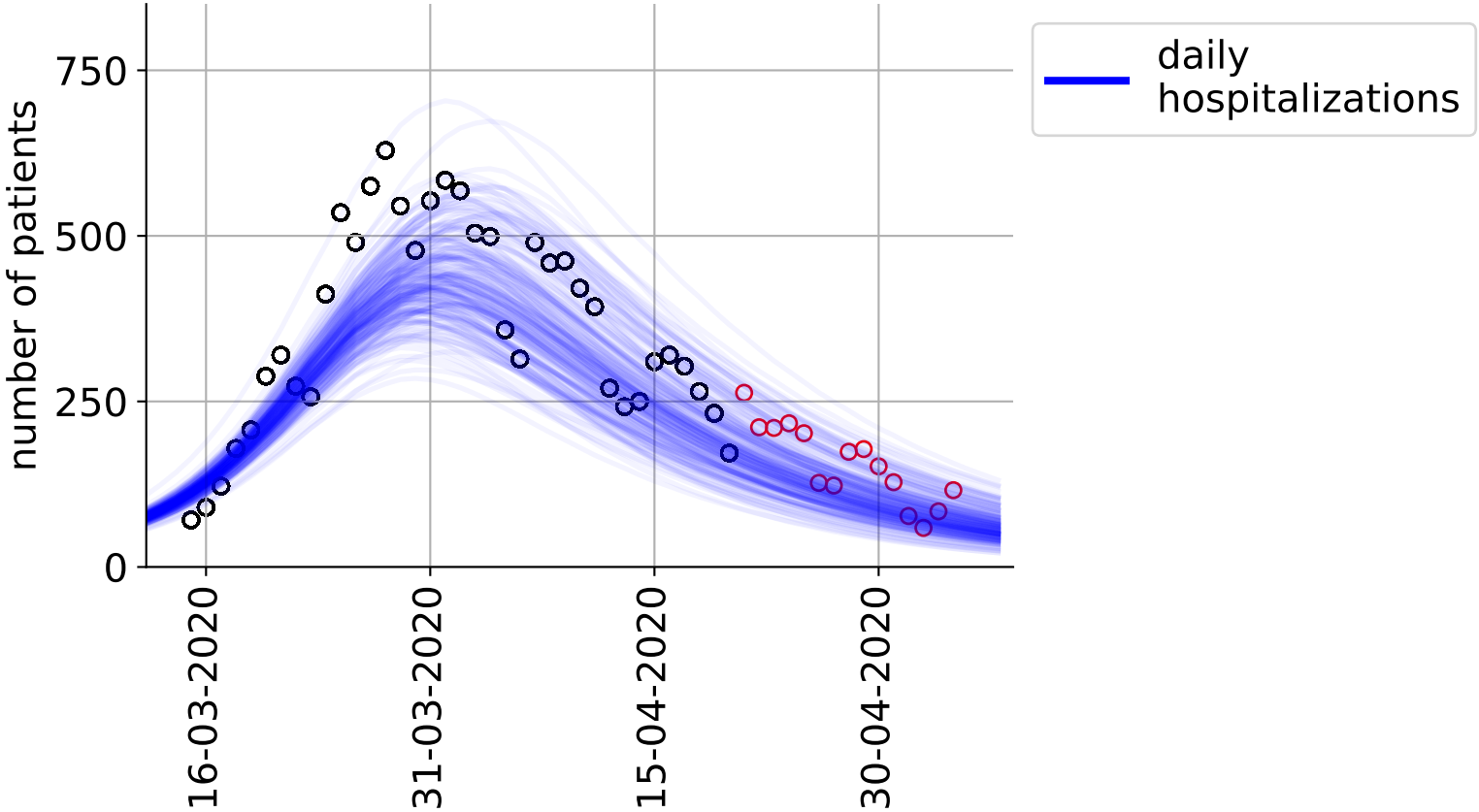
daily hospitalizations
number of patients
750
500
250
0
16-03-2020
31-03-2020
15-04-2020
30-04-2020

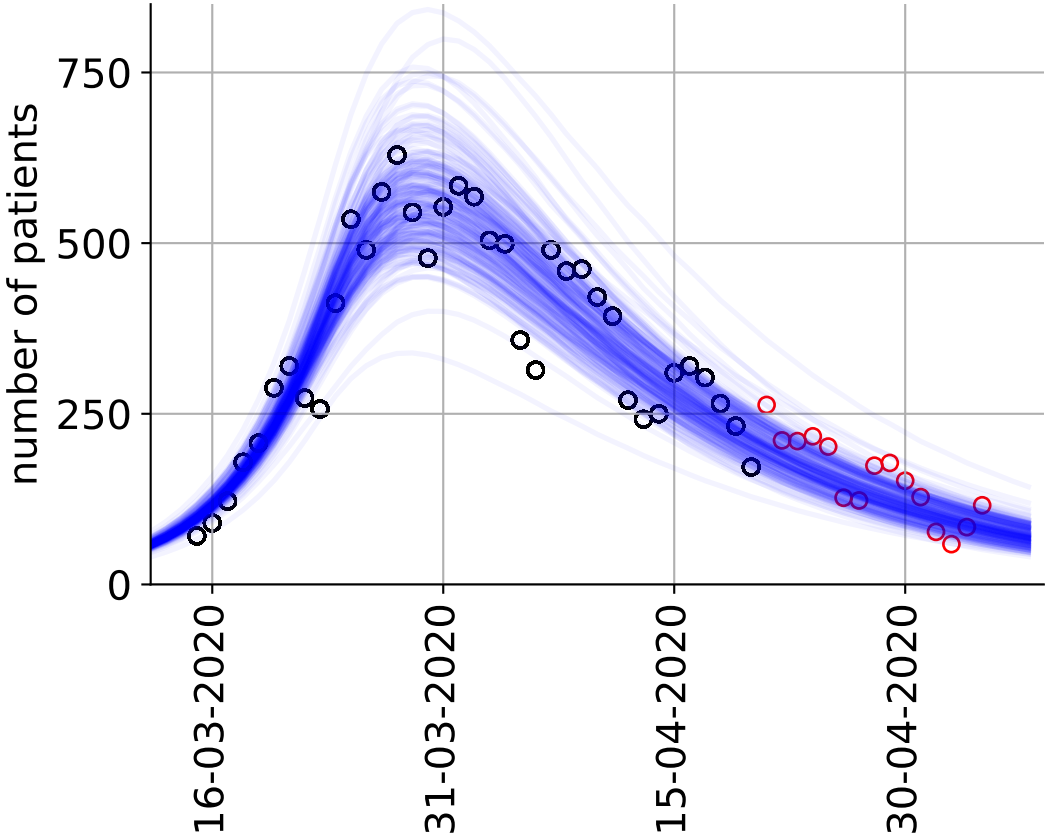
number of patients
750
500
250
0
16-03-2020
31-03-2020
15-04-2020
30-04-2020

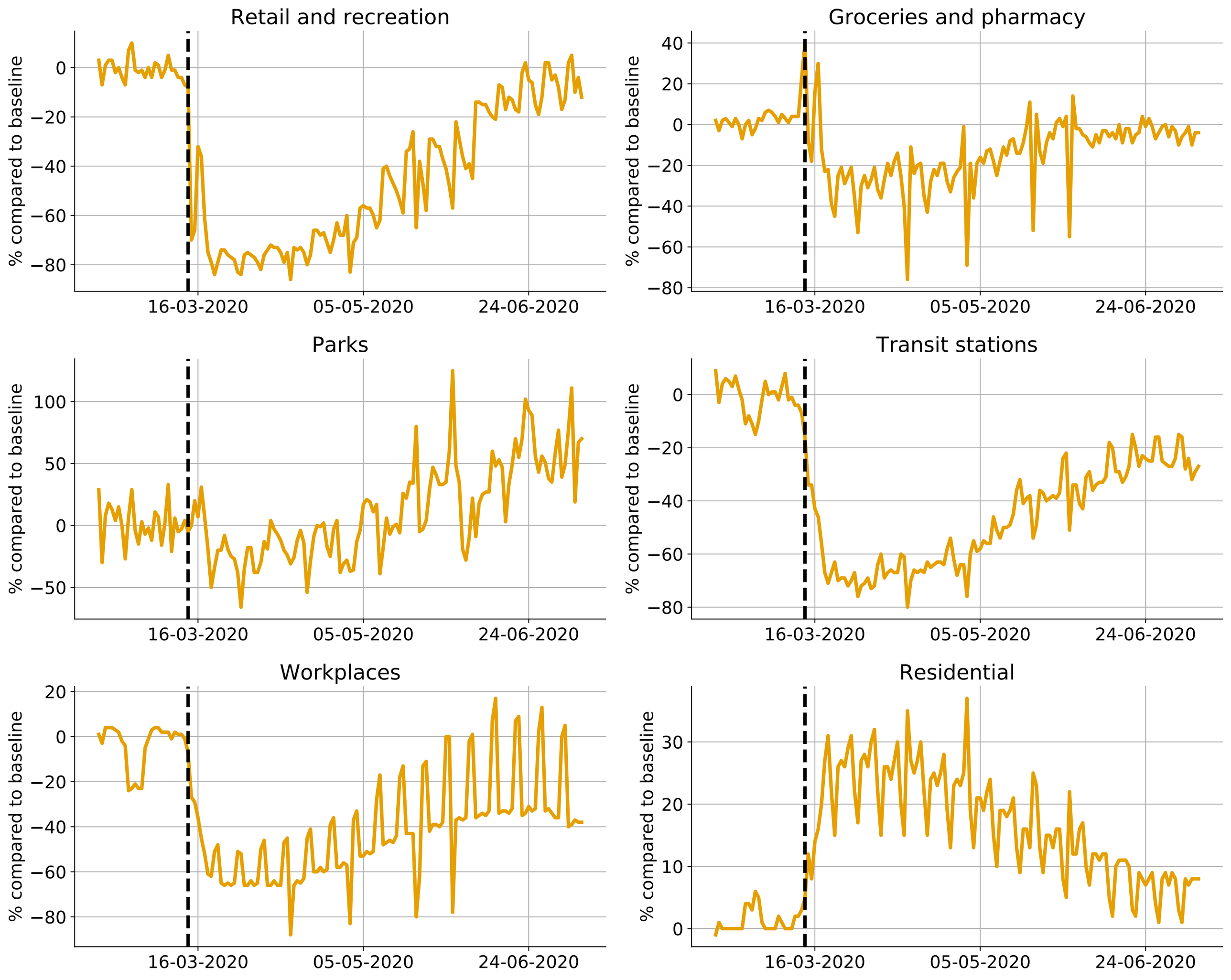
Retail and recreation
% compared to baseline
0
−20
−40
−60
−80
16-03-2020
05-05-2020
24-06-2020
Groceries and pharmacy
% compared to baseline
40
20
0
−20
−40
−60
−80
16-03-2020
05-05-2020
24-06-2020
Parks
% compared to baseline
100
50
0
−50
16-03-2020
05-05-2020
24-06-2020
Transit stations
% compared to baseline
0
−20
−40
−60
−80
16-03-2020
05-05-2020
24-06-2020
Workplaces
% compared to baseline
20
0
−20
−40
−60
−80
16-03-2020
05-05-2020
24-06-2020
Residential
% compared to baseline
30
20
10
0
16-03-2020
05-05-2020
24-06-2020

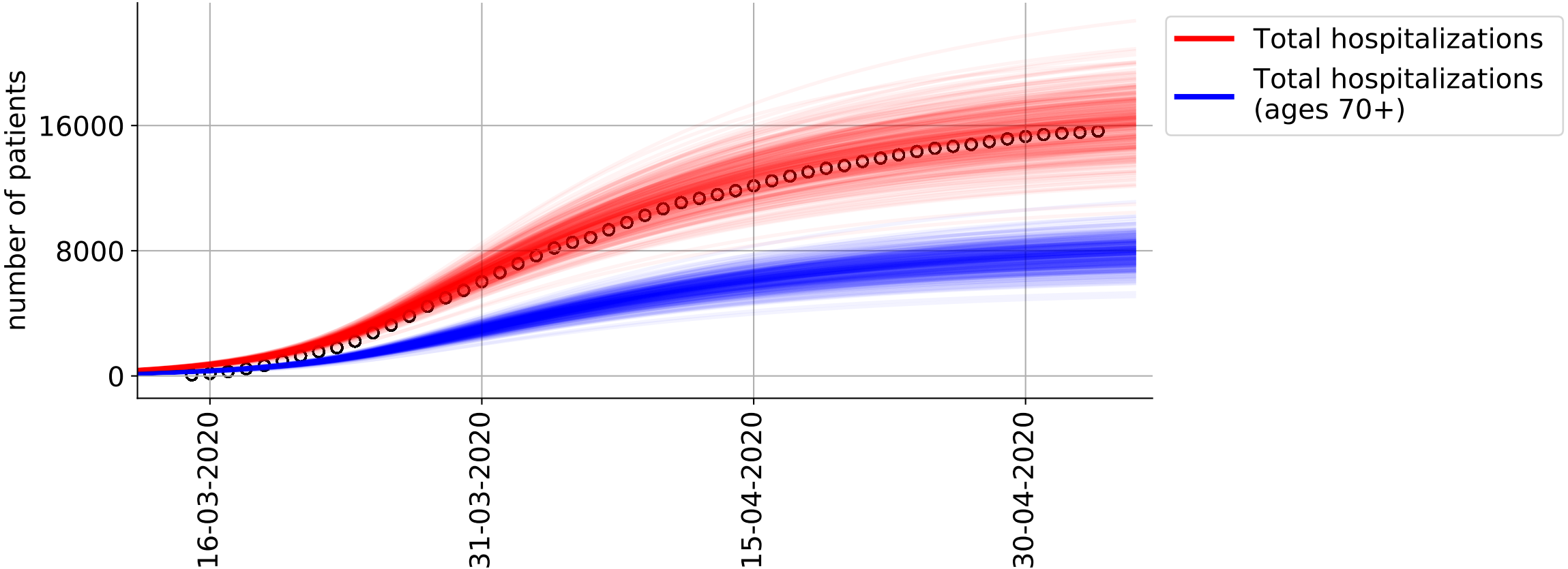
number of patients
16000
8000
0
16-03-2020
31-03-2020
15-04-2020
30-04-2020
Total hospitalizations
Total hospitalizations (ages 70+)

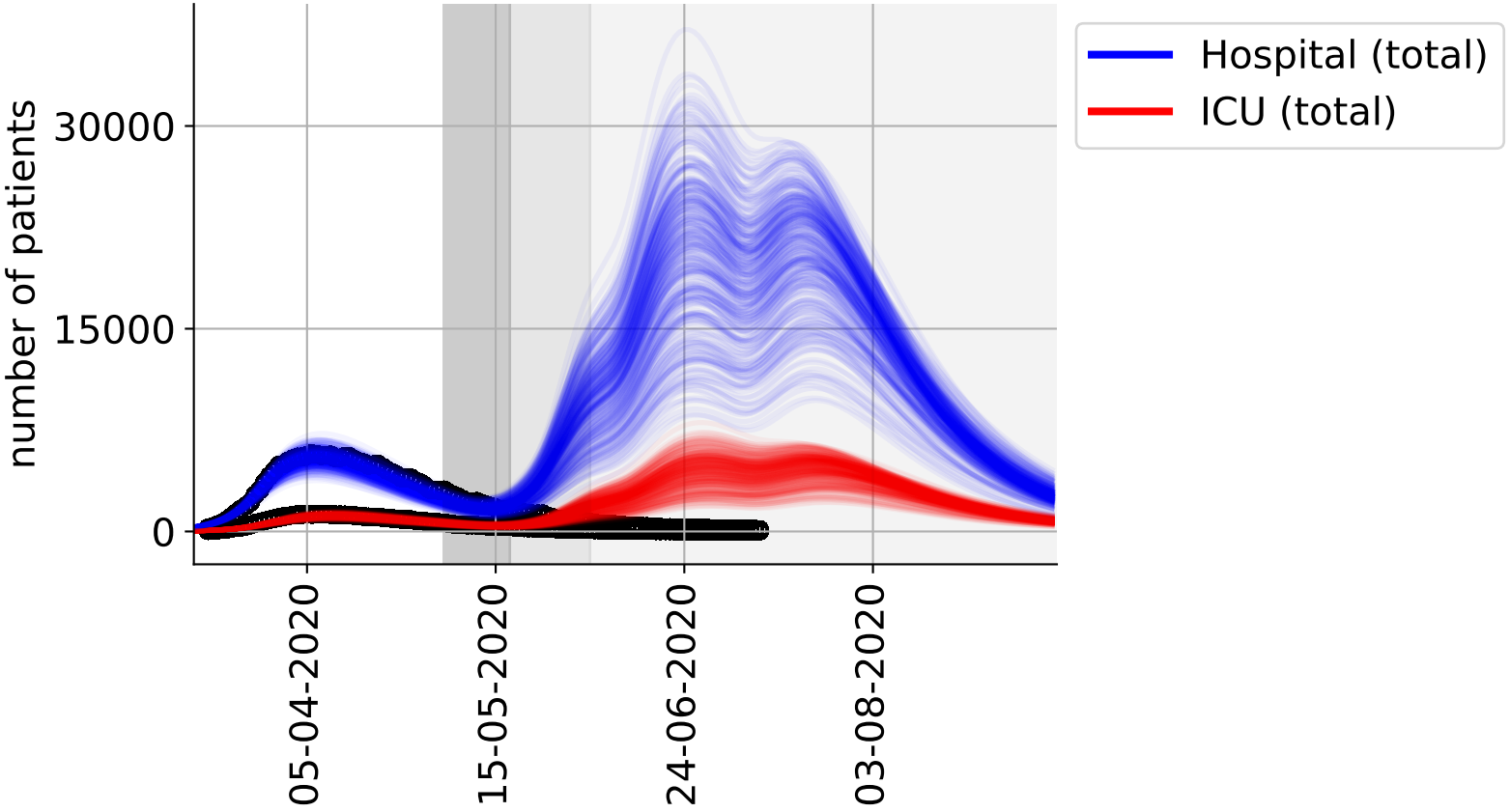
Hospital (total)
ICU (total)
number of patients
30000
15000
0
05-04-2020
15-05-2020
24-06-2020
03-08-2020

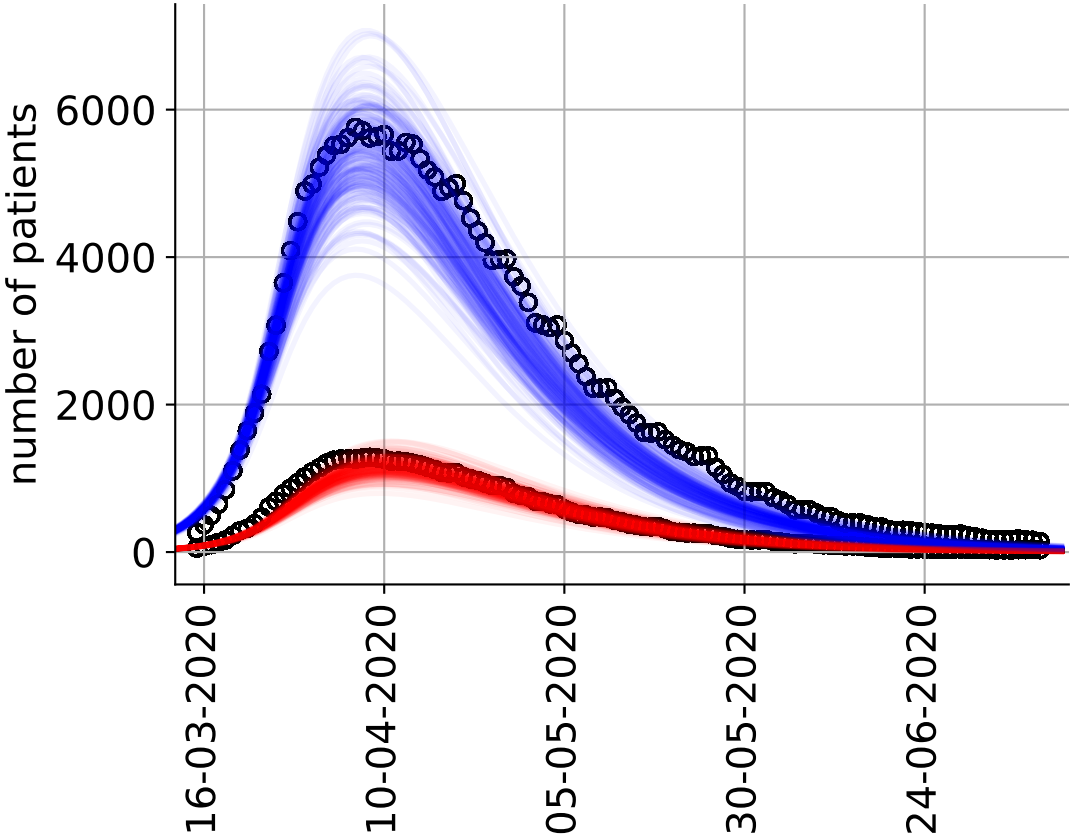
number of patients
6000
4000
2000
0
16-03-2020
10-04-2020
05-05-2020
30-05-2020
24-06-2020